STRUCTURE OF

COLD-ROLLED ALUMINUM

EFFECT OF THICKNESS ON THE STRUCTURE OF

COLD-ROLLED ALUMINUM

By

MICHAEL GEORGE WRIGHT, B.Sc.

A Thesis

Submitted to the Faculty of Graduate Studies

in Partial Fulfilment of the Requirements

for the Degree

Master of Science

McMaster University

February 1964

MASTER OF SCIENCE
(Metallurgy)

McMASTER UNIVERSITY
Hamilton, Ontario

TITLE: Effect of Thickness on the Structure of Cold-Rolled Aluminum.

AUTHOR: Michael George Wright, B.Sc. (University of Wales)

SUPERVISOR: Professor R. K. Ham

NUMBER OF PAGES: vii, 58

SCOPE AND CONTENTS:

The relative merits of methods of determining the density of dislocations are reviewed. In particular, consideration has been given to the evidence available tending to indicate a loss of dislocations from foils of deformed metal during thinning processes preparatory to viewing in the electron microscope. By measurement of the electrical resistivity ratio, 293°K./77°K., during thinning, annealed specimens of super-purity aluminum foil were shown to obey Fuch's theory for thin films, but cold-rolled specimens could not be fitted to the theory. This discrepancy has been attributed to the loss of dislocations from the cold-rolled material, and the results are shown to be consistent with a "loss-fringe" model of dislocation loss from the surface.

ACKNOWLEDGEMENTS

The author is greatly indebted to his supervisor, Dr. R. K. Ham for his continued advice and assistance throughout the duration of this work.

The suggestion for the original experiment arose as the result of discussions between Drs. R. K. Ham, M. H. Loretto and R. L. Segall, and this is acknowledged.

Thanks are also due to Dr. R. G. Ward for the loan of the potentiometer, temperature controller and electric calculator, without which this work would not have been possible; to Division of Tribophysics, University of Melbourne, Australia, for the supply of superpurity aluminum; to the Research Laboratories, Aluminum Company of Canada Limited., and particularly to Dr. R. H. Hay, for their efforts in the rolling of very thin aluminum foil; and to the Research and Development Laboratory, Canadian Westinghouse Company for the loan of tungsten carbide rolls.

This work was carried out with the financial support of the National Research Council, which is gratefully acknowledged.

Table of Contents.

List of Tables

List of Illustrations.

SECTION 1

Introduction

The dislocation as a crystal lattice defect, which could explain the discrepancy between theoretical estimates of the yield strength of metals and the observed values, was introduced as early as 1934 by Taylor (1), Orowan (2) and Polanyi (3). Although other evidence had been put forward to indicate the presence of dislocations in metal crystals, it was with the advent of the thin film technique for use with the electron microscope, that the most detailed evidence was found for the presence of dislocations in metal crystals. In the electron microscope, the dislocations are shown up by a diffraction contrast effect, the strained lattice surrounding the dislocation usually causing enhanced Bragg scattering of the electron beam, hence "magnifying and darkening" the dislocation for view.

Investigations into the production of dislocations, their arrangements into sub-boundaries, and their interaction as an explanation of work-hardening, have stimulated considerable interest in the density of dislocations in a crystalline material. By the use of the electron microscope, it has become possible to view, with a resolution of about 100 $\mathring{A}$., the arrangements of dislocations in materials in various conditions. It is known that cold-worked material possesses many more dislocations than annealed material. Various estimates

have indicated that the difference between annealed and cold-worked copper, for instance, would be about 10^8 cm. of dislocation line per c.c. as compared with 10^{12} cm. of line per c.c.

Various methods have been developed for the measurement of dislocation densities, depending on the change in resistance to an electric current caused by dislocation, the stored energy release on recrystallization, X-ray line broadening, the density change on recrystallization, the magnetic properties of ferromagnetics, work on the strain ageing of iron, and etch pits.

There has been some disagreement in the dislocation density figures obtained from these various sources, and extensive efforts have been and are being made to reconcile the various data. Each estimate, except etch pit data, depends ultimately upon a theoretically deduced property change due to the dislocation, and undoubtedly the discrepancies arise from the various assumptions made in deriving these theoretical property changes, and in applying them to specific cases. However, the direct observation and counting of dislocations in thin films of material by use of the electron microscope does not depend upon any quantitative property of the dislocation, only that it is surrounded by a region of strained lattice which will, under the right conditions, cause enhanced scattering of the electron beam of the microscope.

A recent attempt to reconcile etch pit data and electron microscopy data has been made by Livingston (4). When considered as a function of the resolved shear strain and resolved shear stress, the

dislocation density showed the same general trend in the two data, but the etch pit data was very scattered and varied by a factor of as much as two. The inherent difficulty in this type of correlation is that in the range of dislocation density where the two types of data overlap (10^8 to 10^9 dislocations per cm.^{2}), the density is too low for representative counts to be made in the electron microscope, and too high for the good resolution of etch pits.

Despite new and improved methods of counting, it has been suspected that, especially in terms of dislocation density, thin films are not representative of the bulk material. The very sharp increase in the surface/volume ratio, on thinning the material, might be expected to cause a more than proportional loss of dislocations during the thinning process.

Hirsch (5) has recently summarised the factors which may lead to the underestimation of dislocation densities by means of thin films in the electron microscope. These include the possibility of certain dislocations being invisible due to unfavourable contrast conditions, and the overlapping of images in very dense tangles, and where dislocation boundaries are almost normal to the plane of the film. He also cites four possible types of dislocation rearrangement during thinning, which would result in a net shortening of the dislocation line length in the material.

Ham (6) has attempted to correlate the figures for dislocation density obtained from stored energy measurements by Clarebrough on aluminum, compressed 75%, with his own figures obtained by direct

observation in thin films prepared from the same specimens. The two figures were respectively 3×10^{10} cm.$^{-2}$ and 8×10^{9} cm.$^{-2}$. In an effort to assess this apparent loss of dislocations, Ham prepared thin films of an aluminum-silver alloy. Specimens which were aged prior to thinning showed a higher dislocation density than unaged specimens. Assuming that the ageing precipitate caused pinning of the dislocations and prevention of their loss from the film, this is evidence of a loss of dislocations.

The present work is an attempt to obtain an independent confirmation of this effect by means of electrical resistivity measurements, during the thinning of a metallic foil to a thickness comparable with that for use in the electron microscope.

SECTION 2

Review of Previous Work

This review will consider previous efforts which have been made to determine the dislocation densities of metals, primarily with respect to the method of electrical resistivity measurement. A comparison of measured results with observed densities in thin films has shown up certain discrepancies which tend to indicate that dislocations are lost during the production of the thin film. Consideration is also given to the means by which this may occur.

2.1 Electrical resistivity and the density of dislocations

Two general approaches have been adopted towards the determination of the electrical resistivity change due to a dislocation. The first of these is the purely theoretical approach where workers have attempted to assess the effect of the introduction of a dislocation on the electric field of the lattice, and hence the resistivity that the dislocation causes to the applied current. The other approach has been an experimental one, wherein the dislocation density has been obtained from stored energy or density change measurements during recrystallization, and compared with the simultaneous measurement of the electrical resistivity. Hunter and Nabarro (7) in the first detailed theoretical treatment of the resistivity due to a

dislocation, showed that the strain field in the lattice, surrounding the dislocation, produced very little scattering. The scattering is related to the strain gradient, and is therefore at its greatest at the core of the dislocation, where the treatment was abandoned. These figures have been criticised on the basis of the disadvantages associated with the use of the Born approximation and the linear elastic theory, which was used to calculate the strains. They found a figure of $0.59 \times 10^{-14} N \mu \Omega$ cm.^{3} as the mean resistivity caused by an edge dislocation in copper. N is the density of dislocations in lines per cm.^{2}. They found too, that the resistivity in the slip direction was less than that in the direction perpendicular to the slip plane. The resistivity along the dislocation axis is, of course, zero, as there is no disturbance of the lattice in that direction. This anisotropy ratio varied between 1 and 3, and was found to depend inversely on Poisson's ratio. As Poisson's ratio increased, the anisotropy ratio decreased. The anisotropy figures are in agreement with that of Dexter (8), but are much lower than the 8.3 calculated earlier by Koehler (9). For a screw dislocation, Hunter and Nabarro obtained a figure of $0.18 \times 10^{-14} N \mu \Omega$ cm.^{3}. This is lower than that for an edge dislocation, as a screw dislocation was not thought to cause any dilatation of the lattice.

Seeger and Stehle (10) considered other factors which had been neglected in Hunter and Nabarro's treatment. These arose from non-linearities in the displacements of the atoms and the resulting redistribution of electric charge. This gave no change in the resistivity

due to an edge dislocation, but the resistivity due to the screw dislocation was increased three times over the figure obtained by Hunter and Nabarro.

More recently Seeger and Bross (11) who used a more realistic perturbation potential than is represented by the Born approximation, and who took account of deviations from linear elastic theory, found that scattering by the strain field of an edge dislocation caused a resistivity of $5 - 8 \times 10^{-14} N$ $\mu\Omega$ cm.^{3}, depending upon the cut-off radii employed in the consideration of the strain field.

Harrison (12) has shown that if the core of an edge dislocation is considered to correspond to a line of vacancies, and the resistivity caused by the strain field is neglected, then in copper, the resistivity due to an edge dislocation is about $5 \times 10^{-14} N$ $\mu\Omega$ cm.^{3}.

Adding the contributions due to the core and the strain field would give a maximum possible value of the resistivity due to an edge dislocation of $13 \times 10^{-14} N$ $\mu\Omega$ cm.^{3}.

Concurrently with the theoretical developments, experiments have been carried out to determine the dislocation density in cold-worked materials by a variety of methods; and with a knowledge of the resistivity change on recrystallization, an estimate can be made of the resistivity due to a single dislocation.

Clarebrough, Hargreaves and West (13, 14, 15), and Clarebrough, Hargreaves and Loretto (16, 17) have developed some very accurate differential methods for the determination of the changes in density, stored energy and electrical resistance which occur on recrystalliza-

tion. From their experiments, they calculated the dislocation densities occurring in various cold-worked metals, according to the different properties, employing theoretically deduced values of the property. The main observation from these experiments was that the stored energy data, density data and electrical resistivity data, gave values of the dislocation density in the approximate ratio 1 : 6 : 60, for O.F.H.C. copper (15). The electrical resistivity data was calculated on the basis of Hunter and Nabarro's theory. All three estimates of dislocation density assumed the presence of equal numbers of edge and screw dislocations. It was assumed that in terms of density change, an edge dislocation was equivalent to a line of vacancies of the same length, and that there was no density change due to the removal of a screw dislocation.

They further showed that the density and stored energy results could be reconciled by using the estimates of Stehle and Seeger (18), who had shown that the density change associated with a screw dislocation in copper was not negligible, but equal to between 1 and 2 times the change caused by a line of vacancies of the same length. They further estimated that the density change due to an edge dislocation was greater than that due to a screw. If it was considered that all dislocations caused a density change equivalent to twice that resulting from a row of vacancies of the same length, then the discrepancy between the two sets of results was eliminated. However, data from electrical resistivity measurements still gave dislocation densities of the order of 60 times too large.

The discrepancy still cannot be explained away, even assuming the addition of the effects calculated by Seeger and Bross (11) and by Harrison (12) detailed above.

Initially, it was thought that this discrepancy might be due to micro-fissures in the metal arising from the dilatation side of an edge dislocation. This was worked out in detail by Stroh (19), but it has since been demonstrated by Boas (20), that in order to account for the experimental results, the size of cracks produced would need to be of such a size that they would be readily visible, which they are not.

Broom (21) was probably the first to suggest that a significant contribution could be made to the electrical resistivity of face-centered cubic metals, by stacking faults. Broom and Barrett (22), working with nickel-cobalt alloys found that the maximum resistivity occurred near the transformation composition, where the stacking fault energy would be expected to be low and the faults, correspondingly, relatively wide. The existence of wide faults was confirmed by X-ray diffraction line broadening data. Paterson (23) and Christian and Spreadborough (24) have also shown evidence of the connection between high resistivity and the presence of stacking faults, as shown by X-ray diffraction line broadening.

The effect of a stacking fault ribbon is thought to cause some reflection of conduction electrons. In an early assessment of the effect, Klemens (25) estimated the specular reflection probability for an electron with normal incidence as being about 0.5. More recently (26) he has calculated this value on perturbation theory and obtains a

figure of 0.4. Ziman (27) has pointed out that theoretical attempts to determine this probability by Tweedale (28), and by Blatt, Ham and Koehler (29), have led to probabilities in the range 10^{-3} to 10^{-4}. Seeger (30) has pointed out that even allowing for the fact that the perturbation theory, employed by Klemens, is not very valid for such large probabilities, it is very doubtful that the reflection probability would become as low as 10^{-3}. The observation of stacking faults by contrast in the electron microscope is an indication of their scattering power for high voltage electrons, and it is difficult to see why the same effect would not be experienced by the lower energy conduction electrons. On this basis, the estimate of Klemens would seem to be the more reasonable.

Seeger (31) has estimated that in the cases of copper and nickel, only about 1/40 of the total resistivity is due to the dislocation line itself, the remaining 39/40 being due to the associated fault. Clarebrough et al. (17) have pointed out that to attribute the total discrepancy, between stored energy data and electrical resistivity data, to scattering by stacking faults, requires that in copper faults one atom wide would have to increase the resistivity by an order of magnitude over the undissociated dislocation.

Howie (32) however, has indicated that in aluminum a stacking fault ribbon with a width of one atom spacing would give a resistivity of about $5 \times 10^{-14} N$ $\mu\Omega$ cm.[3].

Even assuming that this can be added to the core and strain field contributions of $13 \times 10^{-14} N$ $\mu\Omega$ cm[3]., to give a total of

18×10^{-14} N $\mu\Omega$ cm.^{3}, the calculated resistivity is still very low compared with the results of Clarebrough et al. (17), namely 33 x 10^{-14} N $\mu\Omega$ cm.^{3}. This discrepancy is even larger if Cotterill's (33) experimental value of (70 ± 20) x 10^{-14} N $\mu\Omega$ cm.^{3} is preferred.

It would appear therefore, that despite these efforts, this problem is still incompletely resolved.

2.2 Thin film electron microscopy and the density of dislocations.

Various methods have been employed for counting dislocations in thin films, notably by Bailey and Hirsch (34). Such procedures are subject to the inaccuracies involved with the invisibility of dislocations lying in certain directions of unfavorable orientation with respect to the surface of the film, and due to the shortening of dislocations during the thinning process by re-orienting themselves in order to lie more normally to the surface of the film, as suggested by Bailey and Hirsch. Ham and Sharpe (35), have shown that this latter effect can be overcome by using a method of surface intersection for counting, rather than the projected area counting of Bailey and Hirsch, or the random line count devised by Ham (36). Ham and Sharpe showed that their technique could increase the observed dislocation density by up to 20%.

Wilsdorf and Schmitz (37), working on aluminum, found that in foils of 4000 Å. thickness, there was a considerable difference in the pattern of dislocations compared with foils of 1200 Å. thickness.

Ham (6) has shown that stored energy measurements by Clarebrough

et. al. (17) on super-purity aluminum compressed 75%, indicate a dislocation density of at least 3×10^{10} cm.$^{-2}$. In electron micrographs of thin films prepared from these specimens, Faulkner and Ham could obtain densities of only 8×10^{9} cm.$^{-2}$. In an attempt to resolve this discrepancy, Ham has carried out experiments on an aluminum -0.5 atomic % silver alloy, in which particles of precipitate (due to the ageing nature of the alloy) were shown to pin dislocations in position, preventing their movement out of the film during thinning. Thin films prepared from aged and unaged alloy indicated a dislocation loss of up to 60% during the thinning operation (electropolishing), or during the early stages of examination of the film in the electron microscope. An additional experiment showed that the ageing effect could not be held responsible for the production of dislocations. Due to the great similarity in the mechanical properties of the supersaturated aluminum - 0.5 atomic % silver alloy and pure aluminum, (atomic diameters: 2.862 Å. for aluminum, 2.888 Å. for silver), it is probably reasonable to infer, as Ham does, that a similar effect would occur with pure aluminum.

Valdrè and Hirsch (38) in some very delicate electron microscopy on stainless steel, have shown that only about 20% of the single dislocations move during or after thinning, and that this movement was usually less than 3,000 Å. The movement of piled up groups of dislocations is not certain, but may have been larger than 3,000 Å. They also showed that the general distribution of the dislocations was very little affected by what movement that took place. This estimate is

somewhat lower than that of Ham. However, this method only permitted observation of the surface, and their estimate was arrived at by inference from these observations.

In a recent review of this problem, Hirsch (5) has summarised the possible means by which movement of dislocations may occur to cause a lowering of the dislocation density during a thinning process. These are:

(a) dislocations running almost parallel to the plane of the film, which tend to rotate to shorten their length. Bailey and Hirsch (34) and Ham and Sharpe (35) have observed this effect, which is estimated at about 20%.

(b) dislocations which end at the same surface, but which thread other dislocations to form nodes, tend to slip out of the surface and remove the node.

(c) dislocation loops near the surface tend to be drawn out of the surface by the image force.

(d) screw dislocations which translate by cross-slip.

Recently, Mader, Seeger and Thieringer (39) have shown that dislocations close to the edge of the foil can escape relatively easily.

Grosskreutz (40) has found that a thin film of aluminum produced by anodizing, contains more dislocations than films produced by the conventional electropolishing technique. This could possibly be associated in some way with the surface strains introduced by adherence of the oxide, causing repulsion of the dislocations from the surface,

and hence no loss of dislocation out from the surface.

From the foregoing, it appears that there can be little doubt that dislocations are lost during the preparation of a thin film. However, in all cases, the evidence has been obtained on the electron microscope using films which had already lost dislocations. No attempt has been made to track the change in dislocation density as thinning proceeds. The present work attempts to do this by employing electrical resistivity measurements to detect the changes.

Although previous workers have found some considerable difficulty in correlating electrical resistivity measurements with other measurements of the dislocation density, this will not interfere with this experiment since it is concerned only with the relative values for a particular specimen.

SECTION 3

Theory

Any experiment which attempts to take account of the various contributions to electrical resistivity in a metal, must involve the so-called "Matthiessen's Rule".

3.1 Matthiessen's Rule.

It was first shown by Matthiessen (41), and by Matthiessen and Vogt (42), that the bulk electrical resistivity at absolute temperature T, $\rho_B(T)$, exhibited by a metal can be considered as the arithmetic sum of two contributions. These arise:-

(a) from the scattering of the conduction electrons by the thermal vibrations, or phonons, of the lattice. This contribution to the resistivity, denoted by ρ_p, is strongly temperature dependent, the resistivity increasing with the temperature, as a result of increased amplitude of atomic vibration (43).

(b) from the scattering of the conduction electrons due to static disturbances resulting from defects in the lattice, such as impurities and variations in long range order, as would be obtained in an alloy. This contribution, ρ_0, is widely considered to be temperature independent.

Matthiessen's Rule may therefore be stated as:-

$$\rho_B(T) = \rho_P(T) + \rho_O$$

As a pure metal is cooled towards $0^\circ K.$, $\rho_P(T)$ will tend to zero as the thermal vibrations of the lattice die away. But, ρ_O, the resistivity due to lattice defects will remain constant down to $0^\circ K.$ This is the so-called "residual resistance".

More up-to-date knowledge of the temperature-independent contribution to electrical resistivity indicates that lattice vacancies, interstitial and impurity atoms, and dislocations, will all scatter the conduction electrons, giving rise to resistivity. For our purposes, we shall include the resistivity contributions due to lattice vacancies, and interstitial and impurity atoms, within the one term ρ_I, and the dislocation contribution within the term ρ_D.

i.e. $\rho_O = \rho_I + \rho_D$

$\therefore \quad \rho_B(T) = \rho_P(T) + \rho_I + \rho_D$

The effect of ρ_I will be considered later.

Mackenzie and Sondheimer (44) have pointed out that at temperatures in excess of the Debye temperature (listed by Kittel (45) as $418^\circ K.$ for aluminum), the phonon scattering of conduction electrons will be very large compared to the scattering caused by dislocations.

Measurements of the electrical resistivity of a pure metal at $20^\circ C.$ ($293^\circ K.$), even if it is not in excess of the Debye temperature, will still consist of a major contribution due to phonon scattering and a minor contribution arising from scattering due to dislocations. At the temperature of liquid nitrogen, $77^\circ K.$, the difference between these contributions will be considerably less, as the reduced thermal

motion of the ions reduces the electron scattering by them.

If any change occurs in the dislocation density, a significant change in the electrical resistivity at 77°K. should be found, and the variation in the ratio:-

$$\frac{\text{electrical resistivity at } 293^{\circ}\text{K.}}{\text{electrical resistivity at } 77^{\circ}\text{K.}}$$

will indicate this change without any knowledge of the dimensions of the specimen.

If during thinning of a foil of metal, there is a decrease in the dislocation density, then an increase should be found in the ratio, due to the effect of the decreased contribution to the electrical resistivity due to the dislocations, being felt more in the denominator than in the numerator.

3.1.1 Validity of Matthiessen's Rule.

Doubts have been expressed as to the validity of Matthiessen's Rule, notably by Basinski, Dugdale and Howie (46) who state that a correction factor should be applied to the rule, especially at temperatures in the range 4.2°K. to 80°K., to allow for the variation in resistivity of dislocations with temperature.

Broom (47) however, has cited various examples of work which has been carried out demonstrating adherence to Matthiessen's Rule, to within about 1% of the resistance considered. However, Bross (48) and Magnusson, Palmer and Koehler (49) have found that in practice, the resistance due to lattice defects is not independent of temperature. In each case the work was performed at temperatures at or near to that of liquid helium. Seeger (50) has shown that Matthiessen's Rule does not

hold at very low temperatures where the dislocations are the main scatterers of conduction electrons.

In a theoretical study, Sondheimer (51) has shown that the residual and ideal resistances are not strictly additive when the two are of the same order of magnitude. In the worst case which he considered, the deviation was less than 1% of the total resistance.

Although the position at the present time is not very clear, it appears that Matthiessen's Rule holds relatively well except at very low temperatures, when the resistance due to the lattice defects becomes of the same order of magnitude as the phonon scattering.

It will be shown that under the most unfavorable of our experimental conditions, the resistance due to dislocations does not rise above 5% of the total resistance.

For our purposes, therefore, we can consider Matthiessen's Rule as being valid.

3.2 Experimental feasibility.

Super-purity aluminum was chosen for these experiments. Previous data obtained by Ham (6) which indicated the loss of dislocations, was from super-purity aluminum (99.991%), and as some of this self-same material was available, it was considered that prior knowledge of the material might prove to be an asset.

Ham (6) has calculated that the stored energy measurements by Clarebrough indicate a dislocation density of 3×10^{10} cm.$^{-2}$ in the bulk material, which had been compressed 75%. This can be considered

as a "saturation" value. Any further cold work would cause very little increase in dislocation density, due to the very effective cross slip mechanism occurring in aluminum, which tends to remove dislocations. In his subsequent work on aluminum-silver alloy, Ham noted that the loss of dislocations appeared to be about 60%.

Assuming the loss of dislocations to be about 50%, i.e. 1.5×10^{10} cm.$^{-2}$, and employing the figure for resistivity due to a dislocation in aluminum as $33 \times 10^{-14} N$ $\mu\Omega$ cm.^{3} (17), we can calculate the resistivity contribution due to lost dislocations as:-

$$\rho_{LD} = 1.5 \times 10^{10} \times 33 \times 10^{-14} \ \mu\Omega \text{ cm.} \quad \text{at } 20^\circ\text{C. } (293^\circ\text{K.})$$
$$= 5 \times 10^{-3} \ \mu\Omega \text{ cm.}$$

This compares with a total resistivity at 20°C. (52) of 2.70 $\mu\Omega$ cm. i.e. the lost dislocations form about .2% of the total resistivity.

An approximate value for the bulk resistivity ratio, $\frac{\rho_B(293)}{\rho_B(77)}$, was readily determined for our material, with the apparatus which will be detailed later, and showed a value of about 10. At 77°K., therefore, we would expect there to be a change in $\rho_B(77)$ of about 2% as a result of losing 50% of the dislocations.

There would therefore be an increase in the resistivity ratio, $\frac{\rho_B(293)}{\rho_B(77)}$ of $(10 - \frac{10.02}{1.02})$ or about 2%.

More recent work by Cotterill (33) gives $(70 \pm 20) \times 10^{-14}$ N $\mu\Omega$ cm.^{3} as the resistivity due to a dislocation in aluminum. The introduction of this figure into the calculation, in place of 33×10^{-14} N $\mu\Omega$ cm.^{3} approximately doubles the increase in the resistivity ratio.

A graph of resistivity ratio against thickness, in the absence of any dislocation loss or other side effects, would have the general form:-

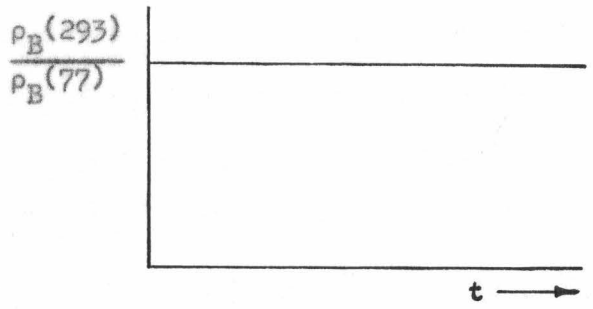

However, when dislocations are lost, this can be expected to be modified to something of the form:-

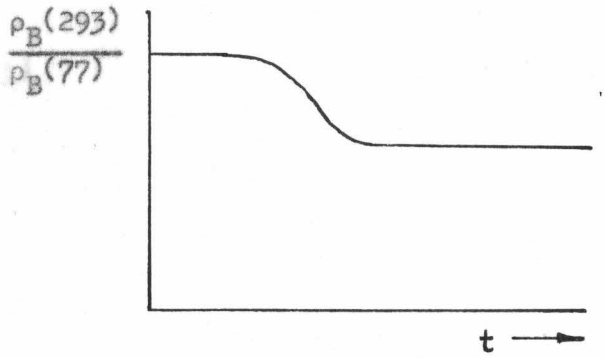

3.3 Effect of other contributions to the resistivity

Other factors which may contribute towards the resistivity are impurity and interstitial atoms, vacancies, and the surfaces of the specimen when it becomes sufficiently thin.

Very pure material eliminates most of the problems of impurity. The use of 99.991% aluminum was of a high enough purity to largely remove all problems associated with inhomogeneity, without being so pure as to permit spontaneous recrystallization on deformation.

The scattering of conduction electrons, by all the above mentioned factors, always has a greater effect in increasing the low temperature resistivity due to the reduced phonon scattering at this temperature. This causes the resistivity ratio to decrease. However, there is no reason to expect that the concentration of vacancies, interstitial or impurity atoms would change during thinning.

Surface scattering of conduction electrons becomes important when the thickness of the specimen becomes of the order of the mean free path of the electrons, so that instead of $\rho_B(T)$, a resistivity $\rho_{total}(T) = \rho_B(T) + \rho_S(T)$, is measured. This assumes that the surface is not perfectly flat. Due to reduced lattice vibration, the mean free path is greater at the lower temperature.

It has been shown by Fuchs (53), that for "thick" films:-

$$\frac{\rho_{total}(T)}{\rho_B(T)} = \frac{\rho_B(T) + \rho_S(T)}{\rho_B(T)} = 1 + \frac{\rho_S(T)}{\rho_B(T)} = 1 + \frac{3}{8K_T}$$

where, ρ_B and ρ_S are the resistivities due to the bulk material, and due to the surface respectively.

where, $K_T = \frac{t}{\ell_T} \frac{\text{(specimen thickness)}}{\text{(mean free path)}} \gg 1$ (for "thick" films).

$$\text{i.e.} \frac{\rho_S(T)}{\rho_B(T)} = \frac{3}{8K_T}$$

Arising from the Sommerfeld Theory, assuming quasi-free electrons, Sondheimer (54) has shown:-

$$\rho_B(T)\ell_T = \frac{h}{\varepsilon^2} \cdot \left(\frac{3}{8\pi}\right)^{\frac{1}{3}} \cdot n^{-\frac{2}{3}}$$

where, n = no. of free electrons - 1.81×10^{23} cm.$^{-3}$ (see Appendix I)

h = Planck's constant - 6.62×10^{-27} erg.sec.

$-\varepsilon$ = electron charge - 1.59×10^{-19} coulomb.

$\rho_B(77)$ bulk resistivity $= 2.70 \times 10^{-7}\ \Omega$ cm.

from which, $\rho_B(77)\ \ell_{77} = 4.05 \times 10^{-12}\ \Omega$ cm.^{2}.

and ℓ_{77}(mean free path at 77°K.) $= .15\ \mu$

Experimental values of $\rho_B \ell$ (55,56) found by matching theoretical curves to data obtained on annealed specimens were found to range from $5.3 \times 10^{-12}\ \Omega$ cm.^{2} to $17.7 \times 10^{-12}\ \Omega$ cm.^{2}. This tends to indicate that an assumption of 3 free electrons per atom (see Appendix I) is not valid in this instance, so that the mean free path is likely to be somewhat larger than the above estimate.

Hence, for a 1 μ film at 77°K.:-

$$K_{77} = \frac{1}{.15} = 6.7 \quad (\gg 1, \text{ as required})$$

$$\therefore \frac{\rho_S(77)}{\rho_B(77)} = \frac{3}{8 \times 6.7} = 5.6 \times 10^{-2}$$

i.e. $\rho_S(77) = 5.6\%$ of $\rho_B(77)$

A similar calculation for 293°K. may be performed, the only difference being the value of 2.70 $\mu\Omega$ cm. for $\rho_B(293)$.

This gives a value of, $\rho_S(293) = .56\%$ of $\rho_B(293)$.

It may be seen, therefore, that the effect of the surface is somewhat greater than, (but of the same order of magnitude as), that to be expected from dislocation loss, but that the change in ratio is a <u>decrease</u>, i.e. it will oppose the effect for which we are looking.

The effect on the graph mentioned above will be such as to cause a change to something of the form:-

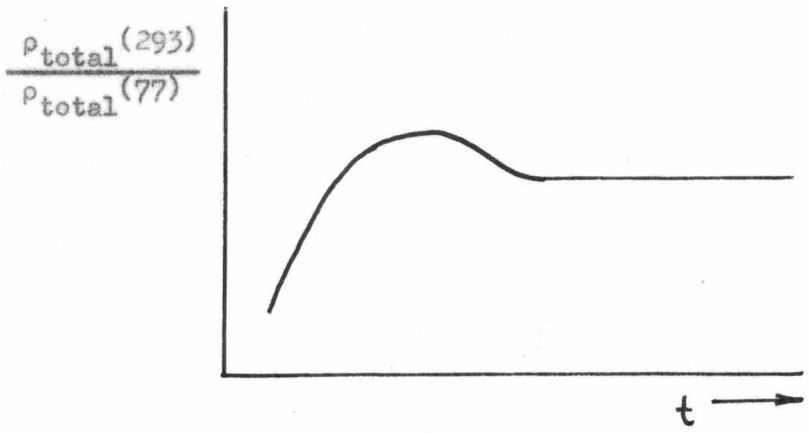

The increase in ratio due to the dislocation loss may or may not be obscured by the surface effect, depending upon the thickness at which it occurs. However, comparison of the graph profile with that of a fully annealed specimen should indicate any relative rise in the graph of the cold-worked specimen due to dislocation loss upon thinning.

SECTION 4

Experimental

4.1 Introduction to the experimental problems.

The three major problems associated with this investigation were concerned with:-

(a) the method of measurement of the electrical resistivity. The low resistances to be anticipated with a metal of high electrical conductivity, such as aluminum, required special circuitry to measure these low resistances. The magnitude of the effect under investigation (2%) required an accuracy of 0.5%, or better in the resistance measurements.

(b) the process used for the even thinning of the film. Even thinning was essential, as any holes in a specimen would contribute significantly to the surface scattering at 77°K. and cause an excessively low resistivity ratio, and an uncontrolled dislocation loss.

(c) the method for measurement of the thickness of the film.

Associated with (a) and (b) was the problem of mounting the specimen to permit both even thinning and resistivity measurements at 20°C. (293°K.) and - 196°C. (77°K.). Part of the mounting problem was the method used for securing the current and potentiometer leads to the specimen foil.

4.2 Material and specimen preparation.

The super-purity aluminum (99.991%) which was used, was supplied by the Aluminum Company of America, in the form of ingots of length 9 cm. and with an equilateral triangular cross-section of side 3 cm.

Sections of one of these ingots, 0.5 cm. thick, were cold rolled to a thickness of 0.010 cm. on a Stanat 2-high rolling mill. Initial attempts to produce thin foil of about 0.001 - 0.0005 cm. were carried out using a 4-high arrangement on the mill with alloy steel work rolls of 1 in, diameter. It was found however, that these rolls were machined with camber to permit the rolling of steel, and rolling a softer material such as aluminum produced center ripple markings in the rolled product. Substantial improvement was obtained with the use of two 3/4 in, diameter work rolls of tungsten carbide. The ripple marks were much reduced, and the higher polish of these rolls imparted a better surface to the product.

Experience showed that for the production of the thin foil the rolls operated best when free of lubricant, and when run at a low speed (about 20 r.p.m.). The use of lubricant and high speeds tended to cause the foils to adhere to the rolls. By rolling foils of about 1 cm. width, it was found that very good specimens could be obtained of width 0.2 - 0.3 cm. by cutting out the center section of the finished ribbon with a razor blade. In this way, foils of 0.0002 cm. were successfully prepared.

In preparing the specimen, the following dimensions were decided upon:

(a) gauge length:- as long as possible from the available piece of rolled foil, in order to increase the resistance. An upper limit of 4 cm. was set, this being the maximum length which could conveniently be thinned.

(b) gauge width:- 0.2 - 0.3 cm. The maximum figure of 0.3 cm. was to ensure a high resistance. 0.2 cm. was considered to be the minimum working width, i.e. anything less than 0.2 cm. was too difficult to handle.

(c) shape:- such that the gauge width of 0.2 - 0.3 cm. was only maintained over the gauge length. The ends were maintained as wide as possible to facilitate the securing of electrical connections.

For ease in mechanical handling, annealed specimens were prepared by annealing the as-rolled foil in air at 400°C. for 17 hr. before cutting out the specimen.

4.3 Mounting of the specimen.

In terms of arrangement of the specimen while tests were carried out, it soon became apparent that there were two conflicting requirements. The first of these was that mechanical handling of the specimen was very difficult, particularly during the thinning procedure, unless it was attached to a support along its entire length. The only satisfactory method which could be found was that it be stuck onto a base plate. Conflicting with this however, was the need to immerse the specimen in a liquid nitrogen bath. No adhesive could be found which did not become brittle at 77°K. However, a commercial

stop-off lacquer, "Miccrostop", used extensively in the specimen preparation for thin film electron microscopy, was found to show a minimum of cracking, and then only after several cycles to 77°K.

The specimen was mounted on a non-conducting "Micarta" board employing "Miccrostop" as an adhesive. This arrangement was found to stand several cycles to 77°K. before further "Miccrostop" was required. This rigid attachment to the base plate caused strain in the specimen at the low temperature due to differential thermal contraction between the specimen and the base plate. Appendix II shows that this strain amounted to some 0.32%, most of which takes the form of plastic extension of the foil in compression. Segall and Partridge (57) have shown that a strain of 0.5%, in super-purity (99.99%), annealed aluminum foil, resulted in a dislocation density increase of considerably less than 5×10^8 cm.$^{-2}$, even allowing for a 50% loss of dislocations from their specimens. This is two orders of magnitude less than the effect that we have measured and in no way affects the results on annealed specimens.

Considerable difficulty was experienced in the obtaining of reliable electrical connections to the specimen foil. Two inherent difficulties were involved. The extremely adherent oxide film was difficult to break up in order to get metal-to-metal contact. In addition, the very thin nature of the specimen made for extreme practical difficulty. Three general contact methods were tried:-

(a) spot welding. This was extremely difficult due to the high thermal conductivity of aluminum and the copper leads. Some success

was achieved by welding the foil to thicker aluminum strip to which the copper leads were attached by alligator clamps. However, due to the inadequacy of the spot welding equipment available, the contacts were electrically unreliable and frequently mechanically weak.

(b) soldering. This was never successful, even in the use of indium and the special solders and fluxes available for soldering aluminum.

(c) pressure contacts. In common with Førsvoll and Holwech (56), it was found that by far the most reliable connection was an ordinary pressure contact. Holes were pierced in the ends of the mounted foil, two in each end, and nuts and bolts passed through. By placing the copper lead under the head of the bolt and holding it, such that it did not turn and apply torque to the specimen, whilst tightening the nut, the lead was forced into the aluminum. Some difficulty was experienced at first with the cold rolled foil, but it was found that this could be overcome by placing a steel block at $77^{\circ}K.$ on the gauge length, while annealing the ends of the specimen with a propane torch.

The ends of the specimen, nuts, bolts and lead wires were coated with "Miccrostop" to prevent attack on them during the thinning procedure. Mechanical stresses were removed from the actual contacts by clamping the lead wires to the base plate with open end hose clamps.

The arrangement of the mounted foil is shown diagrammatically in Fig. 1.

4.4 Measurement of resistance.

In the past, two general methods have been developed for the measurement of resistances of 0.001Ω and less. The first of these is the Kelvin double bridge, as used by Clarebrough et. al. (17) in their measurements on super-purity aluminum. This technique compares two low resistances of similar magnitude by means of a modified Wheatstone bridge. The second method employs a potentiometer to measure the potential drop across the specimen due to an externally applied E.M.F. This method has been used with success by Førsvoll and Holwech (56) and by Cotterill (33). Due to the non-availability of a Kelvin double bridge and a range of standard low resistors, the potentiometric method was chosen.

The electrical circuit employed for the resistance measurement is shown diagrammatically in Fig. 2.

A 600 ampere-hour, 2 volt battery of constant output was used to provide an external E.M.F. which was applied to the specimen through the two outer leads. The potential drop across the specimen was measured via the two inner leads. This method required no knowledge of the resistance of the leads. Thermal E.M.F.s arising from the potentiometer connections were eliminated by the incorporation of a reversing switch.

The only potentiometer available was a Croydon Type P3, which in its low voltage range of 0 - 0.018 volts was only guaranteed accurate to 0.04% or 3μV. whichever was the greater. However, by reading the potential drop at five different current settings and calculating

the resistances, it appeared that the accuracy was rather better than 1 μ V. This was within the accuracy required for the experiment. The potential drop across the potentiometer wire was supplied by a second 2 V. battery, of 200 ampere-hour capacity, which was of very constant output.

In circuit, in series with the specimen, was a 0.1 Ω Manganin wound standard resistor, with a guaranteed accuracy of 0.1(± 0.0005%) Ω at 20°C. An accurate value of the current flowing in the main circuit was obtained by measuring the potential drop across this resistor. The milliammeter was in circuit to provide immediate visual indication of the passage and direction of the current. The wire wound variable step resistor was employed in the circuit for variation of the current. The current reversing switch was a silver contact, four pole, rotary selection device permitting simultaneous reversing of the current in the main circuit and the current in the potentiometer battery circuit.

At each temperature five current settings were employed and the forward and reversed potential drops were measured across both the standard resistor and the specimen. The resistance measurement obtained at each temperature was therefore the average of ten readings.

The temperature bath employed at 293°K. was a water circulator/heater unit. Cold tap water at 9°C. was fed into the unit and the heater adjusted to give 20°C. This unit was guaranteed to give a temperature accurate to ± 0.1°C. No change could be detected on a mercury-in-glass thermometer. The specimen was contained in a rubber bag and lowered into the temperature bath. (see Appendix VI). Resist-

ance measurements were made after one hour, to allow the system to come to equilibrium. The low temperature bath was liquid nitrogen, which remained at its boiling point and gave a constant temperature of 77°K.

Accuracy in the temperatures of both baths was essential. Initial resistance measurements indicated a ratio of about 10, between the resistance at 293°K. and the resistance at 77°K. a difference of 216°K. Hence, a variation in temperature of 0.1°K. would cause a change of about 0.5% in the resistance measurement.

4.5 Thinning procedure.

Three general methods were tried in an effort to thin the rolled film in a uniform manner. These were:-

(a) electropolishing. An extremely good polish was obtained by employing a 1 part perchloric acid : 4 parts methanol solution at 20 volts with a stainless steel cathode. There were, however, two distinct drawbacks to this method.

The first of these was that the edges of the specimen were polished preferentially. This was undoubtedly due to the bunching of the current lines at the edges due to the non-conducting nature of the "Micarta" base plate. An attempt was made to eliminate this problem by the use of an aluminum base plate, from which the specimen was insulated by a thin sheet of mica. This was not satisfactory in operation, probably because of the upraising of the specimen above the base plate. Another attempt was made to overcome this problem by using a P.T.F.E. base plate and stopping off the sides of the specimen with

P.T.F.E. tape. Dewey and Lewis (58) had found that this technique, suitable for the preparation of electron microscope films, eliminated the edge problem with circular specimens of 0.3 cm. diameter. With the long thin specimens which were used here, the results were rather inconclusive. Attack of the edges seemed to have been prevented in certain areas of the specimen, but considerably enhanced in other areas.

The second major draw back was that the rate of polishing was too fast. Trials were made at temperatures down to that where solidification of the electrolyte began, by means of adding liquid nitrogen, but satisfactory results could not be obtained.

An electroetching technique was also tried, employing an electrolyte of 1 part nitric acid : 2 1/2 parts water. A specimen produced in this way for the electron microscope showed a thick oxide layer, and on the basis of Grosskreutz' observations (40), this method was abandoned.

(b) anodising. Following the work of Davies, Friesen and McIntyre (59), who obtained very smooth surfaces on super-purity aluminum by anodising, attempts were made to thin foil by anodising at up to 100 volts in 30 gm./litre ammonium citrate, and removing the oxide layer with a hot solution of orthophosphoric acid and chromium trioxide. The method seemed to work well and was sufficiently slow to allow considerable control over the rate of removal of metal. Unfortunately, microscopic examination of a thinned foil showed a lattice work of very small holes. This would have a great effect in increasing

the surface scattering factor, and for this reason the technique was rejected.

(c) dissolution. Early attempts were made to thin the foil specimens by using an etchant of hydrofluoric acid, and a swabbing technique. This gave very uneven results. Caustic soda was subsequently tried in the same way. The main difficulty was thought to be the fairly high concentration of etchant employed.

By far the most satisfactory method of thinning was by a very low concentration (2 gm./litre) of caustic soda, under constant agitation, into which the specimen was immersed. One micron of thickness could be removed in 45 - 60 min. in this way, and the result was found to be very even. Specimens have been thinned from 7 μ to 1 μ, at the end of which no unevenness could be seen in the specimen.

Due to the nature of the chemical attack, it was thought that preferential attack might occur at the sub-grain boundaries. A "window" specimen for the electron microscope was prepared from as-rolled foil by electropolishing in a perchloric acid-methanol solution. Specimens from this were then placed in 2 gm./litre caustic soda under constant agitation for 10 min. and 30 min. This was equivalent to 20 min. and 60 min. attack from one side only. Figure 3(a) shows an electron micrograph of a thin film produced by electropolishing. Figure 3(b) shows a similar specimen after 30 min. in 2 gm./litre caustic soda. Observation of the thin films in the electron microscope showed no preferential attack for the dislocations in the sub-grain boundaries. The specimens treated in caustic soda differed from the electropolished

specimen in so far as they had extraneous non-metallic material on some areas of the surface, in the form of small specks. This was probably sodium aluminate, $NaAlO_2$, arising from the reaction:-

$$2\ Al + 2NaOH + 2H_2O \longrightarrow 2NaAlO_2 + 3H_2 \uparrow$$

In all cases of solution in caustic soda, gaseous evolution was observed from the specimen, viz. hydrogen.

These specimens also showed some slight, random, localised attack at the edge, which could possibly be associated with impurities. Only one example could be found of etch pits, in apparently random positions, that had been joined by a zig-zag crack.

On the basis of these observations, this was deemed to be a satisfactory method for thinning the specimens.

4.6 Thickness measurement.

In order to determine the thickness at which the dislocation loss occurred, and to enable an estimate to be made of the mechanism involved, some method of thickness measurement was necessary, and this needed to be accurate to 0.5 μ or better.

Due to the necessity of a back plate, micrometer methods were inoperable. The use of X-rays was considered, but calculations indicated that the accuracy obtained was insufficient. (see Appendix III). A possible solution to the problem was the application of β-ray back scattering techniques, but no equipment was available.

Although it was desirable to have an independent method of thickness measurement, it was eventually decided that the simplest

answer to the problem was to employ the room temperature resistance figure, in the relation:-

$$R = \frac{\rho \cdot \ell}{d \cdot t} \quad ,$$

where, R is the room temperature resistance; ρ, the resistivity; ℓ, the length; d, the width and t, the thickness.

A check was made on this method of thickness measurement by using a drum micrometer, which could be read to 0.25 μ, to measure the initial thickness of a specimen, about 13.5 μ in thickness, prior to mounting. It was found that the two methods agreed to about 0.5 μ.

However, the relative measurement of thickness within any one specimen was considerably more accurate. Since no change in width of the specimen during thinning could be detected, the accuracy of the relative thicknesses measured was within .1%.

SECTION 5

Results

Table 1 shows a typical test data sheet, which refers to specimen K2, run 8. The current values were determined from the mean of the potential drops across the standard 0.1 Ω resistor in the forward and reverse positions. The foil resistance was likewise the mean of two potential drops, divided by the current. The resistance figures obtained from the potential drop measurements at five different current values were averaged. The accuracy figures quoted are the standard error of the mean for the five resistance values. The standard error of the mean ratio is the sum of the standard errors for the two individual resistances.

Tables 2 - 8 show the results which were obtained on seven specimens of foil, three of which were tested "as cold rolled", and four after annealing at 400°C. for 17 hr. followed by furnace cooling. The specimen dimensions, length and width, were measured to an accuracy of .025 cm. The dimensions were important for the thickness determination. Any one specimen was self-consistent, as no reduction in surface area was detected in the specimen during thinning. This accuracy was, therefore, important only for the comparison of specimens. Under the worst possible conditions the thickness determined could be in error by 10%.

Figures 4, 5 and 6 show the relationship between resistivity ratio, $\frac{\rho_{total}^{(293)}}{\rho_{total}^{(77)}}$, and thickness, for specimen B2, D2, F2, J2, K2 and L2. They are grouped in pairs to illustrate the difference between specimens in the annealed and cold rolled conditions, commencing at a similar initial thickness.

Over a large range of thickness, the annealed specimens had resistivity ratios in excess of 11.0, as compared with ratios of about 10.0 - 10.5 in the case of cold rolled material. To permit comparison of the two materials, the vertical scales were superimposed, that on the left referring to annealed material, and that on the right to cold rolled material.

In several cases (specimens B2, F2 and L2), cracks appeared in the specimen. These tests were discontinued, as previous experience had shown that cracks gave rise to unrepresentative results.

The technique employed for the resistance measurements was not intended for the determination of resistances of less than .003 Ω, such as were obtained on the thicker specimens, F2 and J2. Consequently the accuracy is very poor at thicknesses in excess of about 12 - 13 μ. This is demonstrated by the limit bars shown in figure 5. The limits represent the standard error of the mean value of the ratio, obtained by addition of the standard errors of the mean values of the resistance at 293°K. and at 77°K. However, at a thickness of 35 μ, an error of 1 μ V. in the potentiometer, between runs, at the extreme low end of its range could give a difference of as much as 1% in the

resistivity ratio between runs. No further account was taken of long term temperature fluctuation of the baths, or other sources of error between runs at different thicknesses.

The relative thickness measurements were accurate to .02% between runs, except again, at high thicknesses.

Specimen H2, shown in figure 7 serves as a check on the general form of the graph for J2, although again the accuracy is poor at the larger thicknesses under consideration.

SECTION 6

Interpretation of results

All seven specimens shown in figures 4 - 7 demonstrate the effect of enhanced conduction electron scattering by the surface at small thicknesses of material. For the purposes of comparison of cold rolled material with annealed material, it was found convenient to group the specimens in pairs commencing at similar initial thicknesses. This demonstrates to better effect the difference in the general forms of the two types of graph.

Figure 4 compares specimen B2 (annealed) with specimen D2 (cold rolled), both of which had an initial thickness of about 8 μ. The annealed specimen showed a rapid fall in the resistivity ratio with decreasing thickness, commencing at the initial thickness. This would be expected from consideration of the surface effect. The cold rolled specimen decreased in ratio much more slowly as the thickness decreased, and the decrease did not become rapid until a thickness of less than 5 μ had been attained. Although the rate of decrease in ratio of the deformed specimen would be expected to be lower due to the lower bulk resistivity ratio, it appears nevertheless, that the rate of fall was sufficiently reduced to indicate the presence of some additional factor which caused the resistivity ratio to remain artificially high.

Figure 6 compares two specimens which were thinned from an

initial thickness of about 14 μ. In this case, the difference between annealed and deformed material was more marked. Although there was a lack of data on specimen L2 (annealed) at the small thicknesses, due to a crack which developed in the specimen, it was evident that the surface effect prevailed at thicknesses up to 14 μ, there being a steadily increasing rate of fall of resistivity ratio as the thickness was decreased. In the deformed specimen (K2), on the other hand, the ratio was observed to remain constant, or even to rise slightly, as the thickness was reduced, before the surface effect became important in the region of 8 - 9 μ, when the ratio decreased in the expected manner. This was a definite indication of some internal change which occurred in the deformed material but not in the annealed material.

Figure 5 compares specimens which were thinned from initial thicknesses in the region of 35 μ. Increases in the resistivity ratio, amounting to as much as 1% were noted in the thickness range 35 μ to 20 μ in annealed and deformed specimens alike. This could not be accounted for, but at these thicknesses the accuracy was very poor, at best being only as good as the scatter bars on the graph. The technique devised for resistivity measurement was not intended to have sufficient accuracy to give representative results in this range of thickness. Nevertheless, the difference between the two specimens was again evident. On the annealed specimen the surface effect became noticeable at a thickness of 20 μ. This was subsequently confirmed by a further specimen (H2, figure 7) which showed the surface effect starting at about 16 μ. The deformed specimen showed no noticeable surface effect

until the thickness had been reduced as low as 10 μ.

These results indicated a significant difference in the electrical conduction behaviour of deformed and annealed material during thinning, commensurate with the expected behaviour when dislocations are lost from the deformed material.

6.1 Determination of bulk mean free path and bulk resistivity ratio for annealed specimens.

In the consideration of annealed material, the resistivity at any temperature may be considered as the sum of resistivity due to the bulk of the metal, and that due to the effect of the surface.

The measured ratio, R, is given by,

$$R = \frac{\rho_{total}(293)}{\rho_{total}(77)} = \frac{\rho_B(293) + \rho_S(293)}{\rho_B(77) + \rho_S(77)}$$

$$\text{i.e. } R = \frac{\rho_B(293) + \rho_S(293)}{\rho_B(293)} \cdot \frac{\rho_B(77)}{\rho_B(77) + \rho_S(77)} \cdot R_B$$

where, R_B is the bulk resistivity ratio, $\frac{\rho_B(293)}{\rho_B(77)}$.

From Sondheimer (54),

$$\frac{\rho_B(T) + \rho_S(T)}{\rho_B(T)} = \left[\frac{\phi(K)}{K}\right]_T$$

$$\therefore \quad R = \left[\frac{\phi(K)}{K}\right]_{293} \cdot \left[\frac{K}{\phi(K)}\right]_{77} \cdot R_B \quad \text{---------} \quad (1)$$

where, $K_T = \dfrac{\text{thickness, } t}{\text{bulk mean free path, } \ell_T}$

and $$\left[\frac{1}{\phi(K)}\right]_T = \frac{1}{K_T} - \frac{3}{4}\left(1 - \frac{1}{12} K_T^2\right) Ei(-K_T) - \frac{3}{8K_T^2}\left(1 - e^{-K_T}\right)$$

$$- \left(\frac{5}{8K_T} + \frac{1}{16} - \frac{K_T}{16} \right) e^{-K_T}$$

where, $Ei\ (-K_T)$ is a tabulated integral of the form:-

$$- Ei\ (-u) = \int_u^{\infty} \frac{e^{-t}}{t} \cdot dt.$$

for which, values were readily available (60).

The limiting form for thick films, i.e. $K_T \gg 1$, is:-

$$\frac{\rho_{B(T)} + \rho_{S(T)}}{\rho_{B(T)}} = 1 + \frac{3}{8K_T} .$$

The limiting form was found to agree, to within .1%, with the full version for $K_T \gg 9$. For values of $K_T < 9$, the full version was employed.

A method of trial and error was used to fit theoretical resistivity ratio versus thickness curves with the experimental curves for annealed specimens B2, H2 and J2. Specimen L2 had an insufficient

number of points, too closely spaced, to allow any success with this method. By setting a value for the bulk resistivity ratio, R_B, and a value for the bulk mean free path, ℓ_{77}, the resistivity ratios at various thicknesses could be determined.

Example.

Specimen H2

Assume: bulk resistivity ratio, $R_B = 11.34$

bulk mean free path at $77^\circ K$, $\ell_{77} = .40\ \mu$

specimen thickness, $t = 4\ \mu$.

From section 3.3

$\rho_B \ell$ = constant, assuming the same number of free electrons throughout.

$$\therefore \quad \ell_{293} = \frac{\ell_{77}}{R_B} = \frac{.40}{11.34}\ \mu = .0353\ \mu.$$

$$K_{77} = \frac{4}{.40} = 10$$

$$K_{293} = \frac{4}{.0353} = 113.4$$

From the theory outlined above, $\left[\frac{\phi(K)}{K}\right]_{77} = 1.039$

$$\left[\frac{\phi(K)}{K}\right]_{293} = 1.0033$$

From (1),

$$R = \frac{1.0033}{1.039} \times 11.34$$

$$= 10.947$$

By suitably adjusting the values of ℓ_{77} and R_B, a good curve fit was obtained for specimen B2, and for specimens H2 and J2 up to the maxima of the curves. The theoretical curves are shown as solid lines in figures 4, 5 and 7. The results are outlined in table 9.

$\rho_{B(77)}$ was calculated from the bulk resistivity ratio, assuming that $\rho_{B(293)} = 2.7\ \mu\Omega$ cm. (52). $\rho_B\ell$ was then readily obtained.

The curves for the annealed specimens were found to fit Fuchs' theory over the whole range of thickness considered, but the cold rolled specimens could not be made to fit the theory over the same range for any value of R_B and ℓ_{77}.

If it is assumed that $\rho_B\ell$ is the same for the cold rolled specimens as for the annealed specimens, then Fuchs' curves may be calculated to compare with experimental curves for cold rolled specimens. Obviously, the theoretical curve and the experimental curve would start from the same ratio at the initial thickness.

6.2 Determination of bulk resistivity ratio for cold rolled material.

$$\frac{\rho_{B(293)}}{\rho_{B(77)}} = R_B, \qquad \rho_{B(77)} = \frac{2.70 \times 10^{-6}}{R_B}\ \Omega \text{ cm.}$$

Employing the mean value of $\rho_B \ell$ which was determined above, (see table 9),

$$\ell_{77} = \frac{12.6 \times 10^{-12} \times R_B}{2.70 \times 10^{-6}} \text{cm.} = \left[.0467 \times R_B\right] \mu$$

$$\ell_{293} = .0467\ \mu \quad \text{(from table 9).}$$

Consider specimen D2.

Commencing thickness: 8.38 μ

Ratio measured: 10.14

From (1) above, $R = \left[\frac{\phi(K)}{K}\right]_{293} \cdot \left[\frac{K}{\phi(K)}\right]_{77} \cdot R_B \cdot$

At 8.38 μ, $K_{77} = \frac{8.38 \times 10^{-4}}{.0467 \times R_B} = \frac{179.43}{R_B}$

From previous experience we know that R_B will be about 10 or 11.

$\therefore K_T > 9$ and the short formula may be used with an accuracy of better than .1%.

$$\therefore \left[\frac{\phi(K)}{K}\right]_{77} = 1 + \frac{3R_B}{8 \times 179.34} = \frac{(1435.44 + 3R_B)}{1435.44}$$

At 8.38 μ, $K_{293} = \frac{8.38 \times 10^{-4}}{.0467} = 179.43$

Again, $K_T > 9$, $\therefore \left[\frac{\phi(K)}{K}\right]_{293} = 1 + \frac{3}{8 \times 179.43} = \frac{1438.44}{1435.44}$

From (1),

$$R = \frac{1438.44}{1435.44} \times \frac{1435.44}{(1435.44 + 3R_B)} \times R_B$$

but, $R = 10.14$

$\therefore R_B = 10.337$

i.e. bulk resistivity ratio for specimen D2 = 10.337.

A similar calculation for specimen K2 led to a value of 10.341.

6.3 Determination of dislocation loss on thinning.

A specimen of cold rolled material, assuming no dislocation loss on thinning, would follow a resistivity ratio versus thickness curve dictated by the values of $\rho_B \ell$ and the bulk resistivity ratio. Theoretical curves were obtained for specimens D2 and K2 by the determination of points according to the method shown in section 6.1.

Figures 8 and 9 show the comparisons of the experimental and theoretical curves for specimens D2 and K2 respectively. In each case an 80% confidence limit is shown for the theoretical curve, i.e. an 80% confidence limit for $\rho_B \ell$ from the annealed specimens. These are shown as dotted lines in the figures, and in each case the experimental curves can be seen to lie outside these limits, at higher resistivity ratios than would be expected. This is in agreement with the effect to be expected when dislocations are lost from the specimen.

The resistivity ratio for the theoretical curve, i.e. for cold rolled material, assuming no dislocation loss on thinning, is:-

$$R = \frac{\rho_B(293) + \rho_S(293) + \rho_D}{\rho_B(77) + \rho_S(77) + \rho_D} \quad \text{- - - - - - - - -} \quad (2)$$

where ρ_D is the resistivity contribution due to the dislocations, assumed to be independent of temperature (see section 3.1).

For the experimental curve, i.e. cold rolled material, assuming some loss of dislocations on thinning:-

$$R^1 = \frac{\rho_B(293) + \rho_S(293) + \rho_D^1}{\rho_B(77) + \rho_S(77) + \rho_D^1} \quad \text{- - - - - - - - -} \quad (3)$$

where ρ_D^1 refers to the resistivity caused by the prevailing number of dislocations in the specimen.

Neglecting the resistivity contribution due to dislocations at 293°K. which is only about 0.5% of the total resistivity at 293°K.

From (2),

$$\rho_B(77) + \rho_S(77) = \frac{\rho_B(293) + \rho_S(293)}{R} - \rho_D$$

Substituting in (3),

$$R^1 = \frac{\rho_B(293) + \rho_S(293)}{\frac{\rho_B(293) + \rho_S(293)}{R} - \left[\rho_D - \rho^1{}_D\right]}$$

The loss of resistivity caused by dislocations $= \left[\rho_D - \rho^1{}_D\right] = \Delta\rho_D$.

$$\Delta\rho_D = \left[\rho_B(293) + \rho_S(293)\right] \left[\frac{1}{R} - \frac{1}{R^1}\right] \quad \text{- - - - - -} \quad (4)$$

It may be seen, therefore, that the loss of resistivity due to dislocations is dependent upon the vertical separation of the theoretical and experimental curves.

Considering specimen K2, at a thickness of 1.6 μ, it may be

seen from figure 9 that the respective values of R and R^1 are 9.28 and 9.69.

Equating, $\left[\rho_B(293) + \rho_S(293)\right]$ to 2.70 $\mu\Omega$ cm.

by substitution in (4),

$$\Delta\rho_D = 2.70 \left[\frac{1}{9.28} - \frac{1}{9.69}\right] \mu\Omega \text{ cm.}$$

$$= 1.23 \times 10^{-2} \ \mu\Omega \text{ cm.}$$

By a series of these calculations the curves of $\Delta\rho_D$ versus thickness, for specimens D2 and K2, shown in figure 10, were obtained.

At any thickness, the difference in the average density of dislocations between the experimental case and the theoretical case is obtained from the relevant $\Delta\rho_D$ value using an assumed resistivity for a unit dislocation.

Employing the result of Clarebrough et. al. (17) for the resistivity due to a dislocation in aluminum as 33×10^{-14} N $\mu\Omega$ cm.^{3}, the loss in dislocation density of specimen K2 at a thickness of 1.6 μ is:-

$$\frac{1.23 \times 10^{-2}}{33 \times 10^{-14}} \text{ cm.}^{-2}.$$

$$= 3.78 \times 10^{10} \text{ cm.}^{-2}$$

Employing Cotterill's (33) more recent value for the resistivity due to a dislocation in aluminum, $(70 \pm 20) \times 10^{-14}$ N $\mu\Omega$ cm.^{3},

the loss of dislocation density varies from: 1.38×10^{10} cm.$^{-2}$ to 2.48×10^{10} cm.$^{-2}$.

SECTION 7

Discussion.

Comparison of the experimental data with that to be expected theoretically indicates the presence in the cold rolled specimens of some factor causing an artificially high resistivity ratio as thinning proceeds. This may be accounted for, (a) by a gain in resistivity at 293°K., due to an increase in the number or efficiency of scattering centres for the conduction electrons, but which do not cause an increase, or a considerably smaller increase in resistivity at 77°K., or (b), by a decrease in the number or efficiency of scattering centres, occurring exclusively or predominantly at 77°K.

The temperature dependent factors causing resistivity may change their temperature dependence on thinning due to a change occurring in the phonon spectrum or in the atomic vibration modes of the surface atoms. However, we do not think that this is important at the thickness considered; also, it is difficult to see why cold rolled specimens should be different from annealed specimens. The underlying cause for the increase must therefore be connected with the temperature independent scattering contributions. In the face of Matthiessen's Rule, which shows that all temperature independent contributions to resistivity have a greater effect at lower temperatures, possibility (a) appears to be precluded. Possibility (b), however, is in support

of Matthiessen's Rule, as a loss of temperature independent scattering centers from the specimen on thinning, a loss which is not proportional to the thickness of the specimen, would cause the observed effect.

The only temperature independent scattering centres thought to be present in the specimens were dislocations, lattice vacancies, and interstitial and impurity atoms. There is no evidence available to suggest that point defects, such as vacancies, interstitials and impurities would be lost from a material during thinning, on any basis other than one proportional to the thickness. At the temperatures employed in this work any interstitials and vacancies produced in the deformation process would anneal out. Impurity atoms depend upon diffusion for movement, and the rate at which this occurs is sufficiently low for the process to be neglected.

Dislocations however, are line defects, possessing line tensions, which can cause a reduction in line length when restraining effects are removed. When a specimen containing dislocations is thinned, rearrangements may occur which cause a reduction in dislocation line length and therefore a lowering of the contribution to resistivity due to the dislocations. According to Matthiessen's Rule, this change has a greater effect on the total resistivity at $77^{\circ}K.$ than at $293^{\circ}K.$, thus causing an increase in the resistivity ratio.

Figure 10 shows a continuous increase in the loss of resistivity due to dislocations over the range of thickness under consideration. Electron microscopy (61) has shown that no consistent change in dislocation density could be found on thinning from .7 μ to .1 μ. At

low thicknesses therefore, the graphs would be expected to level off somewhat due to a reduced dislocation loss. This seems to be indicated by the shape of the lower confidence limit in both cases.

At large thicknesses, the graphs of figure 10 would be expected to become parallel to the thickness axis at $\Delta\rho_D = 0$, when the thickness is sufficiently great for the dislocation rearrangement at the surface on thinning to have a negligible effect on the total resistivity. The fact that our graphs are far from parallel to the thickness axis at the high thickness end is an indication of the fact that a loss of dislocations had occurred from the starting material before the test commenced, i.e. dislocations were being lost from the foil during the rolling stage. Due to the nature of our experimental equipment, insufficiently accurate data was obtained at the higher thickness values.

These results are in keeping with a mechanism envisaged of a front of dislocation loss gradually advancing into the foil as thinning proceeds. This mechanism has been developed theoretically (see Appendix IV). The curves thus derived have been fitted to the experimental curves of $\Delta\rho_D$ versus thickness for specimens D2 and K2. This is shown in figure 11.

The reason for the poor fit of the experimental and theoretical curves at higher thicknesses is uncertain, but is probably due to experimental error. It could however, be caused by some inhomogeneity in dislocation density introduced into the material as a result of the deformation process.

Electron micrographs of the foil were taken, e.g. figure 12, and the sub-grain size was determined according to the method of Smith and Guttman (62), assuming "spherical" grains. This gave a value of 1.54 μ as the sub-grain size. Assuming that the fringes of dislocation loss from the specimen are half a sub-grain size in thickness, and employing Cotterill's (33) value for the resistivity due to a dislocation, the loss of dislocations may be assessed from the derived equation of Appendix IV.

With the prior knowledge of the minimum dislocation density of the same material, due to Ham (6), as 8×10^{9} cm.$^{-2}$, the percentage dislocation loss on thinning to less than one sub-grain thickness was determined. This amounted to 54% in the case of specimen D2 and 76% in the case of specimen K2. This is in excellent agreement with the results of Ham (6) who calculated a 60% loss. This agreement must to some extent at least, be regarded as fortuitous, considering the experimental error involved, and the difference in initial dislocation density of 1.75×10^{10} cm.$^{-2}$ for specimen D2, and 3.4×10^{10} cm.$^{-2}$ for specimen K2.

The assumption of a loss fringe width of half a sub-grain thickness seems reasonable, since the removal of a portion of the sub-grain would be expected to allow the dislocations associated with the sub-grain to spill out, effectively reducing the density of dislocations in the specimen as a whole. An arbitrary plane cutting an assembly of sub-grains would "open" the metal to an average depth of half a sub-grain on either side of the cut.

This "loss fringe" model can take account of the mechanisms proposed for dislocation loss on thinning by Hirsch (5), all of which depend upon the close proximity of a surface. However, it appears from these results that no significant loss of dislocations could be detected by electron microscopy in the presence of a sub-grain size greater than the penetration depth of the electron beam. This accounts for Ham's (61) observation in the electron microscope which showed no loss on thinning from .7 μ to .1 μ.

It should be noted however, that the energy of a dislocation in aluminum must be less than 3.53×10^{-4} ergs/cm., if dislocations in aluminum are to lie in less energetic configurations than dislocations in silver (see Appendix V). This is to be expected on the basis of the much easier cross-slip and polygonization in aluminum than in silver.

From Clarebrough et. al. (17) energy measurements, we must then find that the bulk dislocation density for aluminum is more than 3.4×10^{10} cm.$^{-2}$. From the resistivity measurements of Clarebrough et. al. (17) we find that the electrical resistivity due to a dislocation is less than 38×10^{-14} N μΩ cm.^{3}, in disagreement with Cotterill's (33) value of $(70 \pm 20) \times 10^{-14}$N μΩ cm.^{3} Cotterill's result may be too high because of dislocation loops lost on thinning which he did not allow for sufficiently.

Therefore, the dislocation loss may be as high as 72% for specimen D2 and 87% for specimen K2. These last results are still consistent with the 60% found by Ham (6), since his method could only give a lower limit to the dislocation loss.

SECTION 8

Conclusions.

1. This investigation has shown that thin films of deformed super-purity aluminum do not obey Fuchs' theory for the effect of thickness on electrical resistivity. Annealed specimens were shown to obey this theory.

2. The lack of obedience to Fuchs' theory could not be accounted for by any temperature dependent scattering centre, or by any temperature independent scattering centre other than dislocations.

3. The results obtained are consistent with a theory involving a "loss front" of dislocations, one half sub-grain in thickness, moving into the specimen during thinning.

4. The magnitude of the dislocation loss on thinning of deformed aluminum, 54% and 76%, determined on separate specimens, is in agreement with the only other assessment of the effect, viz. 60%.

SECTION 9

Implications of the "loss fringe" Hypothesis and Suggestions for Future Work

The improvement of the above mentioned technique, by the application of more accurate temperature controlling equipment and a more sensitive potentiometer, should permit a more definite and accurate assessment of the "loss fringe" model which has been proposed, particularly at low thicknesses.

Considerable caution must be exercised in applying these results to other metals and even to differing purities of the same metal, since variation in such factors as sub-grain size, impurity, precipitates and atomic structure must all be taken into account.

Nevertheless in the light of the present results, the validity of the technique of thin film electron microscopy for metals other than aluminum should be examined, since whatever the sub-grain size in the material, a considerable portion of the thickness of the film will consist of "loss fringe" material. However, the presence of precipitates or impurities will tend to hold the dislocations in the foil, and a material showing a large Peierls force will tend to lose dislocations less readily than such metals as aluminum. The sub-grain size of a metal generally becomes smaller

as the amount of deformation is increased, so that the depth of the "loss front" should decrease. Therefore thin films from heavily deformed material should lose fewer dislocations during thinning than thin films from lightly deformed material.

Etch pit data should also, on the basis of the present results be considered as suspect, from the point of view of the dislocation densities which are obtained. One method of approach which may work to give evidence of the "loss front" model would be to pin the dislocations in the material, for instance by the addition of zinc to copper. Silver, in particular, would be a good material with which to work due to the high resolution etch pit techniques now available for this metal. By the dissolution of successive layers and making dislocation density determinations by etch pit methods at each stage, some increase in the dislocation density should be found, assuming that the pinning mechanism does not contribute significantly to the number of etch pits in any other way.

The validity of the theories of stage II work hardening which are presently held, are supposed to be strongly supported by the experimental finding, by both thin film and etch pit methods, of $\sigma \propto N^{1/2}$, where σ is the flow stress and N the dislocation density, increasing with increasing deformation. If the "loss fringe" model applied to the metals for which this relation has been established, the relation may be fortuitous, and should be re-examined and if possible corrected (e.g. by using the pinned-dislocation model suggested above). Indirect measurements, as discussed in section 2.1, in

general indicate a higher dislocation density than thin films and etch pits do for the same flow stress. This would be expected on the basis of the present results.

Appendix I.

Free electrons in aluminum

The atomic packing of aluminum is of the face-centered cubic form, having 4 atoms to each unit cell.

The unit cell size is given by Barrett (Structure of Metals, 1952, McGraw-Hill), as 4.049 $\mathring{A}$.

$$\text{No. of atoms per c.c.} = \frac{4}{(4.049 \times 10^{-8})^3}$$

$$= 6.03 \times 10^{22}$$

The latest work on aluminum, by Ziman (The Fermi Surface, 1960, J. Wiley & Sons), suggests that all three outermost electrons in each atom may be considered as being free and available for conduction.

$\therefore$ no. of free electrons = 1.81×10^{23} cm.$^{-3}$.

Appendix II.

Strain in the mounted specimen

(Data are taken from "Handbook of Chemistry and Physics", 43rd. edn.).

Coefficient of linear thermal expansion of aluminum, $= 18.35 \times 10^{-6}$ per $^{\circ}C$.

Decrease in length of a 4 cm. specimen on cooling, $293^{\circ}K$. to $77^{\circ}K$.

$= 4 \times 18.35 \times 10^{-6} \times (293 - 77)$ cm.

$= .01585$ cm.

Coefficient of linear thermal expansion of Micarta 32 X, $= 33 \times 10^{-6}$ per $^{\circ}C$.

Decrease in length of Micarta over 4 cm. gauge length, on cooling, $293^{\circ}K$. to $77^{\circ}K$. $= 4 \times 33 \times 10^{-6} \times (293 - 77)$ cm.

$= .02851$ cm.

$$\text{Strain in aluminum} = \frac{.02851 - .01585}{4}$$

$= .317\%$.

Modulus of elasticity of aluminum, 10^7 p.s.i.

Strain of .317% corresponds to a stress of $10^7 \times .00317$ p.s.i.

$= 3.17 \times 10^4$ p.s.i

This is considerably in excess of the yield stress of 1.88×10^4 p.s.i., and therefore takes the form of plastic extension.

Appendix III.

Accuracy of X-ray thickness measurement of aluminum.

For X-rays passing through a thin sheet of material, the following relation holds:- $I_t = I_o e^{-\mu t}$

where, I_t is the transmitted X-ray intensity

I_o is the incident X-ray intensity

μ is the absorption coefficient

t is the thickness.

For two thicknesses, t_1 and t_2, 0.5 μ different (the minimum accuracy required), the ratio of transmitted intensities would be:-

$$\frac{I_2}{I_1} = e^{-\mu(t_2 - t_1)}.$$

For the CuK_α radiation available, μ for aluminum is given by Barrett (Structure of Metals, 1952, McGraw-Hill) as 18.02.

$$\therefore \frac{I_2}{I_1} = e^{18.02 \times 0.5 \times 10^{-4}}$$

$$= e^{.0009}$$

$$\frac{I_2}{I_1} = 1.0009$$

A discrimination of better than 0.09% is required between the two intensities.

Employing a scintillation counter and an extremely high intensity giving a large count, say 10^6 pulses, the probable error involved is approximately $\sqrt{10^6}$, or 10^3 pulses.

This represents an accuracy of 0.1%.

Although this is almost accurate enough for our purpose, it must be remembered that some absorption would be involved with the "Micarta" base plate, and variation in the incident beam could be as high as 0.1%, particularly as the series of measurements for thickness would be made over a considerable period of time.

Appendix IV.

Dislocation loss mechanism

Consider a specimen of length ℓ, width w and thickness t.

Suppose that there is a front of dislocation loss advancing inwards from each side, a constant distance t_o from the edge, such that the dislocation density at the centre of the foil, N_1 is reduced discontinuously to a density N_2 at a distance t_o from the outside edge of the foil.

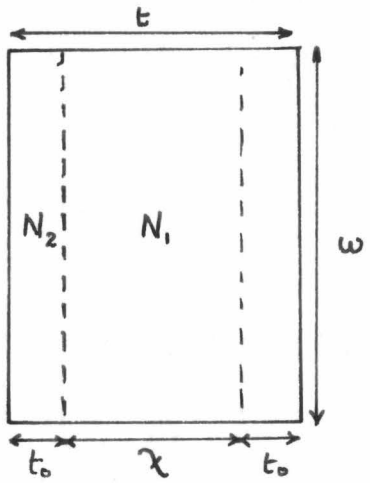

Assume that $w \gg t$ in order that loss from the side ℓ, t is very small compared with loss from the side ℓ, w.

Resistivity due to dislocations, $\rho_D = C \times \frac{S}{V}$ $\frac{\text{(dislocation line length)}}{\text{(volume)}}$

where, C = resistivity due to a single dislocation.

Dislocation line length in central zone, $S_1 = x\, w\, \ell\, N_1$

Dislocation line length in outer zone, $S_2 = 2t_o\, w\, \ell\, N_2$

Total dislocation line length, $S = S_1 + S_2$

$$= w \ \ell \ (\chi N_1 + 2t_o N_2)$$

$$\therefore \quad \rho_D(t) = C \times \frac{(\chi N_1 + 2t_o N_2) \ w \ \ell}{(\chi + 2t_o) \ w \ \ell} = C \times \frac{(t - 2t_o)N_1 + 2t_o N_2}{t}$$

The change in resistivity due to dislocation loss on thinning from a thickness t_1 to a thickness t, is:-

$$\Delta\rho = \rho_D(t_1) - \rho_D(t)$$

$$= C.N_1 - C. \frac{2t_o}{t_1} . (N_1 - N_2) - C.N_1 + C . \frac{2t_o}{t} (N_1 - N_2).$$

$$= C.2t_o(N_1 - N_2) \left[\frac{1}{t} - \frac{1}{t_1}\right].$$

Using the known value of C, and assuming the value of $2t_o$ as 1.54 μ (t_o = 1/2 the sub-grain thickness), with t_1 equal to the starting thickness of the specimen concerned, $(N_1 - N_2)$ the dislocation loss, can be adjusted so that the curve fits well with the experimental curve (see Figure 11).

Appendix V.

Correlation of electrical resistivity and stored energy measurements.

From Clarebrough et. al. (17), for aluminum,

Change in resistivity upon annealing 75% compressed aluminum,

$\Delta \rho_D$ = .013 $\mu \Omega$ cm.

Stored energy released on annealing 75% compressed aluminum,

= .119 cal./gm.

∴ Energy of dislocation line, from above value, and Faulkner and Ham's (63) determination of $N = 8 \times 10^9$ lines/cm.^{2} using thin films, gives 17.1×10^{-4} erg./cm. dislocation line.

But, for silver, (Bailey and Hirsch (34))

$$\frac{\text{Stored energy measured}}{\text{Thin film dislocation density}} = 4.5 \times 10^{-4} \text{ erg./cm. dis/}^{n}\text{. line.}$$

$$\text{Energy of dislocation} = \frac{\mu b^2}{K} \log_e \left(\frac{R}{r}\right).$$

where, μ is the shear modulus, b the Burger's vector, K is 4π for a screw dislocation and $4\pi(1 - \nu)$ for an edge dislocation, where v is Poisson's Ratio, R and r are cut-off radii in consideration of the strain field.

	Silver	Aluminum	
μ	2.9×10^{11} dynes/cm.^{2}	2.7×10^{11} dynes/cm.^{2}	
ν	0.38	0.34	
b	2.88 Å.	2.86 Å.	
μb^2	2.405	2.210	. . . . . (a)
$\frac{\mu b^2}{(1-\nu)}$	3.880	3.345	. . . . . (b)
Mean: [of (a) and (b)]	3.14	2.78	

For silver, energy of dislocation = 4.5×10^{-4} erg./cm.

$$\text{Configuration factor} = \frac{4.5 \times 10^{-4}}{3.14} = 1.43 \times 10^{-4}.$$

For Al, expect a configuration factor of less than 1.43×10^{-4}.

$\therefore$ energy of dislocation in aluminum $< 1.43 \times 10^{-4} \times 2.78$ erg./cm.

i.e $< 3.98 \times 10^{-4}$ erg./cm.

This is expected because aluminum can cross slip and polygonize more easily than silver.

Hence, dislocation density $> 3.4 \times 10^{10}$ cm.$^{-2}$.

$\therefore$ resistivity due to a single dislocation

$$< \frac{.013}{3.4 \times 10^{10}} \; N \mu \Omega \text{cm.}^3$$

i.e. $< 38 \times 10^{-14} \; N \mu \Omega$ cm.^{3}

(Data from: Metals Reference Book, C. J. Smithells, Butterworths, 1962)

Appendix VI.

Temperature bath difficulties

Initially the room temperature bath employed mineral oil into which the specimen was placed without any intermediate covering. It was subsequently discovered however, on repeat tests at the same thickness, that an increase in resistance occurred which was caused by an attack on the specimen by components of the oil. The oil was changed for high purity dibutyl phthalate and although the discrepancy was reduced, attack on the specimen still occurred. This was ruled down to attack of the aluminum by trichloroethylene, which was used for degreasing after removal from the dibutyl phthalate.

An alcohol bath was substituted for the oil bath, but obnoxious fumes, evaporation loss and water pick up, made this technique undesirable, and it was decided that a water bath should be used with the specimen placed inside a flexible container before immersion.

REFERENCES

1. Taylor, G. I., 1934, Proc. Roy. Soc., A 145, 362.
2. Orowan, E., 1934, Zeit. Phys., 89, 605, 614, 634.
3. Polanyi, M., 1934, Zeit. Phys., 89, 660.
4. Livingston, J. D., 1962, Acta Met., 10, 229.
5. Hirsch, P. B., 1963, Report on Conference on the Relation between Structure and Strength in Metals and Alloys, National Physical Laboratory, Teddington, Jan. 1963.
6. Ham, R. K., 1962, Phil. Mag., 7, 1177.
7. Hunter, S. C. and Nabarro, F. R. N., 1953, Proc. Roy. Soc., A220, 542.
8. Dexter, D. L., 1952, Phys. Rev., 86, 770.
9. Koehler, J. S., 1949, Phys. Rev., 75, 106.
10. Seeger, A. and Stehle, H., 1956, Zeit. Phys., 146, 242.
11. Seeger, A. and Bross, H., 1960, Zeit. Naturf., 15A, 663.
12. Harrison, W. A., 1958, J. Phys. Chem. Solids, 5, 44.
13. Clarebrough, L. M., Hargreaves, M. E. and West, G. W., 1955, Proc. Roy. Soc., A232, 252.
14. Clarebrough, L. M., Hargreaves, M. E. and West, G. W., 1956, Phil. Mag. 1, 528.
15. Clarebrough, L. M., Hargreaves, M. E. and West, G. W., 1957 Acta Met., 5, 738.

16. Clarebrough, L. M., Hargreaves, M. E. and Loretto, M. H., 1960 Proc. Roy. Soc., A257, 363.

17. Clarebrough, L. M., Hargreaves, M. E. and Loretto, M. H., 1961, Phil. Mag., 6, 807.

18. Stehle, H. and Seeger, A., 1956, Zeit. Phys., 146, 217.

19. Stroh, A. N., 1957, Adv. in Phys., 6, 418.

20. Boas, W., 1956, Conference on Dislocations and Mechanical Properties, Lake Placid, New York. p. 342.

21. Broom, T., 1952, Proc. Phys. Soc. (London), B65, 871.

22. Broom, T. and Barrett, C. S., 1953, Acta Met., 1, 305.

23. Paterson, M. S., 1952, J. App. Phys., 23, 805.

24. Christian, J. W. and Spreadborough, J., 1956, Phil. Mag., 1, 1069.

25. Klemens, P. G., 1953, Australian J. Phys., 6, 122.

26. Klemens, P. G., 1956, Canadian J. Phys., 34, 1212.

27. Ziman, J. M., 1956, Discussion on (26).

28. Tweedale, cited in discussion on (26).

29. Blatt, F. J., Ham, F. S. and Koehler, J. S., 1956, Bull. Amer. Phys. Soc., 1, 114.

30. Seeger, A., 1956, Canadian J. Phys., 34, 1219.

31. Seeger, A., 1956, Conference on Dislocations and Mechanical Properties, Lake Placid, New York. p. 348.

32. Howie, A., 1960, Phil. Mag., 5, 251.

33. Cotterill, R. M. J., 1963, Phil. Mag., 8, 1937.

34. Bailey, J. E. and Hirsch, P. B., 1960, Phil. Mag., 5, 485.

35. Ham, R. K. and Sharpe, N. G., 1961, Phil. Mag., 6, 1193.

36. Ham, R. K., 1961, Phil. Mag., 6, 1183.

37. Wilsdorf, H. G. F. and Schmitz, J., 1962, J. App. Phys., 33, 1750.

38. Valdrè, U. and Hirsch, P. B., 1963, Phil. Mag., 8, 237.

39. Mader, S., Seeger, A. and Thieringer, H. M., 1963, Report on Conference on the Relation between Structure and Strength in Metals and Alloys, National Physical Laboratory, Teddington, Jan. 1963.

40. Grosskreutz, J. C., 1963, Private communication.

41. Matthiessen, A., 1860, Ann. Phys. Chem. Lpz., 110, 190.

42. Matthiessen, A. and Vogt, G., 1864, Ann. Phys. Lpz., 7, 761, 892.

43. Mott, N. F. and Jones, H., 1936, Theory of the Properties of Metals and Alloys, Oxford University Press, London.

44. Mackenzie, J. K. and Sondheimer, E. H., 1949, Phys. Rev., 77, 264.

45. Kittel, C., 1960, Introduction to Solid State Physics, Wiley, New York.

46. Basinski, Z. S., Dugdale, J. S. and Howie, A., 1963, Phil. Mag., 8, 1989.

47. Broom, T., 1954, Adv. In Phys., 3, 26.

48. Bross, H., 1959, Zeit. Naturf., 14A, 560.

49. Magnusson, G. D., Palmer, W. and Koehler, J. S., 1958, Phys. Rev., 109, 1990.

50. Seeger, A., 1956, Conference on Dislocations and Mechanical Properties, Lake Placid, New York., p. 504.

51. Sondheimer, E. H., 1950, Proc. Roy. Soc., A203, 75.

52. Clarebrough, L. M., 1962, Private communication.

53. Fuchs, K., 1938, Proc. Camb. Phil. Soc., 34, 100.

54. Sondheimer, E. H., 1952, Adv. in Phys., 1, 1.

55. Montariol, F. and Reich, R., 1962, Comptes Rendus, 254, 3357.

56. Førsvoll, K. and Holwech, I., 1963, J. App. Phys., 34, 2230.

57. Segall, R. L. and Partridge, P. G., 1959, Phil. Mag., 4, 912.

58. Dewey, M. A. P. and Lewis, T. G., 1963, J. Sci. Instr., 40, 385.

59. Davies, J. A., Friesen, J. and McIntyre, J. D., 1960, Canadian J. Chemistry, 38, 1526.

60. Jahnke, E. and Emde, F., Tables of Functions, 4th edn. Dover, New York.

61. Ham, R. K., 1962, Unpublished work.

62. Smith, C. S. and Guttman, L., 1953, J. Metals, 5, 81.

63. Faulkner, E. A. and Ham, R. K., 1962, Phil. Mag., 7, 279.

TABLE 1 Typical test data sheet.

Specimen K2. Run 8. Resistivity ratio: 10.12

Temperature 293°K. Accuracy: .03%

Rheostat setting	Potential drop 0.1Ω resistor		Potential drop Specimen		Current	Foil resistance
Ω	forward	reverse	forward	reverse	amp.	Ω
40	4.964	4.963	4.551	4.549	.049635	.0916692
30	6.547	6.546	6.002	6.000	.065465	.0916673
25	7.794	7.791	7.145	7.142	.077925	.0916715
20	9.620	9.616	8.818	8.815	.096180	.0916687
15	12.563	12.560	11.518	11.514	.125615	.0916769

Average value: .0916703

Accuracy: .002%

Temperature 77°K.

Rheostat setting	Potential drop 0.1Ω resistor		Potential drop Specimen		Current	Foil resistance
Ω	forward	reverse	forward	reverse	amp.	Ω
40	4.980	4.979	.451	.450	.049795	.0090471
30	6.578	6.575	.596	.595	.065765	.0090550
25	7.834	7.831	.710	.709	.078325	.0090584
20	9.681	9.678	.878	.876	.096795	.0090604
15	12.667	12.664	1.148	1.146	.126655	.0090561

Average value: .0090554

Accuracy: .024%

TABLE 2 Resistance measurements on specimen B2.

Annealed Condition — Length: 3.550 cm.

17 hr. 400°C. Furnace Cooled — Width: .250 cm.

Run No.	Resistance 293°K.	Resistance 77°K.	Resistivity Ratio	Standard Error of Mean Ratio	Thickness
	Ω	Ω		%	μ
1	.0529170	.0046812	11.304	.08	7.26
2	.0527686	.0046882	11.256	.05	7.26
3	.0571702	.0050823	11.249	.04	6.71
4	.0569656	.0050835	11.206	.04	6.71
5	.0619913	.0055205	11.229	.05	6.15
6	.0617721	.0055278	11.175	.05	6.15
7	.0628295	.0056357	11.148	.06	6.15
8	.0629125	.0056369	11.161	.06	6.15
9	.0690452	.0061889	11.156	.05	5.55
10	.0690380	.0061919	11.150	.04	5.55
11	.0761121	.0068565	11.101	.02	5.04
12	.0761578	.0068801	11.069	.04	5.04
13	.0846300	.0076495	11.063	.05	4.53
14	.0846556	.0076556	11.058	.04	4.53
15	.0956208	.0086970	10.995	.03	4.01
16	.0956199	.0087036	10.986	.04	4.01
17	.1097559	.0101023	10.864	.04	3.49
18	.1100259	.0101188	10.873	.05	3.49
19	.1302007	.0122199	10.655	.04	2.95
20	.1305015	.0122544	10.649	.04	2.95

TABLE 3 Resistance measurements on specimen D2.

Cold Rolled Condition

Length: 3.550 cm.

Width: .250 cm.

Run No.	Resistance 293°K.	Resistance 77°K.	Resistivity Ratio	Standard Error of Mean Ratio	Thickness
	Ω	Ω		%	μ
1	.0457820	.0045071	10.158	.04	8.38
2	.0514572	.0050982	10.093	.04	7.45
3	.0569957	.0056476	10.092	.06	6.72
4	.0631790	.0062906	10.043	.04	6.07
5	.0710147	.0070544	10.067	.03	5.40
6	.0835757	.0083222	10.043	.04	4.59
7	.0991625	.0099611	9.955	.04	3.87
8	.1213407	.0122959	9.868	.01	3.16
9	.1513815	.0155167	9.756	.02	2.54

TABLE 4 Resistance measurements on specimen F2.

Cold Rolled Condition

Length: 3.850 cm.

Width: .225 cm.

Run No.	Resistance 293°K.	Resistance 77°K.	Resistivity Ratio	Standard Error of Mean Ratio	Thickness
	Ω	Ω		%	μ
1	.0147785	.0014512	10.184	.13	31.26
2	.0181033	.0017808	10.166	.18	25.52
3	.0227438	.0022210	10.240	.13	20.32
4	.0284455	.0027720	10.262	.09	16.24
5	.0356505	.0034720	10.268	.07	12.96
6	.0460787	.0044851	10.274	.04	10.02
7	.0618362	.0060488	10.223	.07	7.47

TABLE 5 Resistance measurements on specimen H2.

Annealed Condition — Length: 3.450 cm.

17 hr. 400°C. Furnace Cooled — Width: .300 cm.

Run No.	Resistance 293°K.	Resistance 77°K.	Resistivity Ratio	Standard Error of Mean Ratio	Thickness
	Ω	Ω		%	μ
1	.0096737	.0008645	11.190	.14	32.09
2	.0101237	.0009100	11.125	.11	30.67
3	.0126108	.0011310	11.150	.08	24.62
4	.0160227	.0014328	11.183	.17	19.38
5	.0202346	.0018029	11.223	.08	15.35
6	.0269163	.0024043	11.195	.04	11.54
7	.0353408	.0031646	11.168	.05	8.79
8	.0462877	.0041772	11.081	.05	6.70
9	.0600320	.0054229	11.070	.05	5.17
10	.0865334	.0079795	10.844	.01	3.59

TABLE 6 Resistance measurements on specimen J2.

Annealed Condition — Length: 3.975 cm.

17 hr. 400°C. Furnace Cooled — Width: .250 cm.

Run No.	Resistance 293°K.	Resistance 77°K.	Resistivity Ratio	Standard Error of Mean Ratio	Thickness
	Ω	Ω		%	μ
1	.0119505	.0010637	11.234	.06	35.92
2	.0121324	.0010797	11.237	.11	35.39
3	.0139480	.0012419	11.231	.16	30.78
4	.0167155	.0014836	11.267	.12	25.69
5	.0209463	.0018506	11.319	.13	20.49
6	.0209628	.0018551	11.300	.18	20.49
7	.0283917	.0025148	11.290	.08	15.12
8	.0421328	.0037430	11.256	.03	10.19
9	.0869101	.0079510	10.931	.04	4.94

TABLE 7 Resistance measurements on specimen K2.

Cold Rolled Condition

Length: 3.900 cm.

Width: .250 cm.

Run No.	Resistance 293°K.	Resistance 77°K.	Resistivity Ratio	Standard Error of Mean Ratio	Thickness
	Ω	Ω		%	μ
1	.0305455	.0029919	10.209	.03	13.79
2	.0312920	.0030533	10.249	.05	13.46
3	.0356628	.0034916	10.214	.04	11.81
4	.0411583	.0040084	10.268	.04	10.24
5	.0484556	.0047321	10.240	.04	8.70
6	.0574610	.0056257	10.214	.05	7.33
7	.0722678	.0071127	10.160	.02	5.83
8	.0916703	.0090554	10.123	.03	4.60
9	.1173369	.00116591	10.064	.02	3.59
10	.1655353	.00166376	9.949	.01	2.55
11	.2774424	.0286818	9.673	.01	1.52

TABLE 8 Resistance measurements on specimen L2.

Annealed Condition — Length: 3.700 cm.

17 hr. 400°C. Furnace Cooled. — Width: .275 cm.

Run No.	Resistance 293°K.	Resistance 77°K.	Resistivity Ratio	Standard Error of Mean Ratio	Thickness
	Ω	Ω		%	μ
1	.0266697	.0023016	11.587	.06	13.62
2	.0273876	.0023846	11.485	.05	13.26
3	.0307448	.0026878	11.439	.11	11.82
4	.0353500	.0031051	11.384	.05	10.28
5	.0416558	.0037013	11.254	.03	8.72
6	.0497204	.0044554	11.160	.04	7.31

TABLE 9 Results of curve fitting for annealed specimens.

Specimen	Bulk resistivity ratio R_B	Bulk mean free path at 77°K. ℓ_{77}	Bulk mean free path at 293°K. ℓ_{293}	Bulk resistivity at 77°K. $\rho_{B(77)}$	$\rho_B \ell$
Units		μ	μ	$\times 10^{-7}$ Ω cm.	$\times 10^{-12}$ Ω cm.^{2}
B2	11.64	.66	.0567	2.32	15.3
H2	11.34	.40	.0353	2.38	9.5
J2	11.47	.55	.0480	2.35	12.9
Mean values	11.48	.54	.0467	2.35	12.6

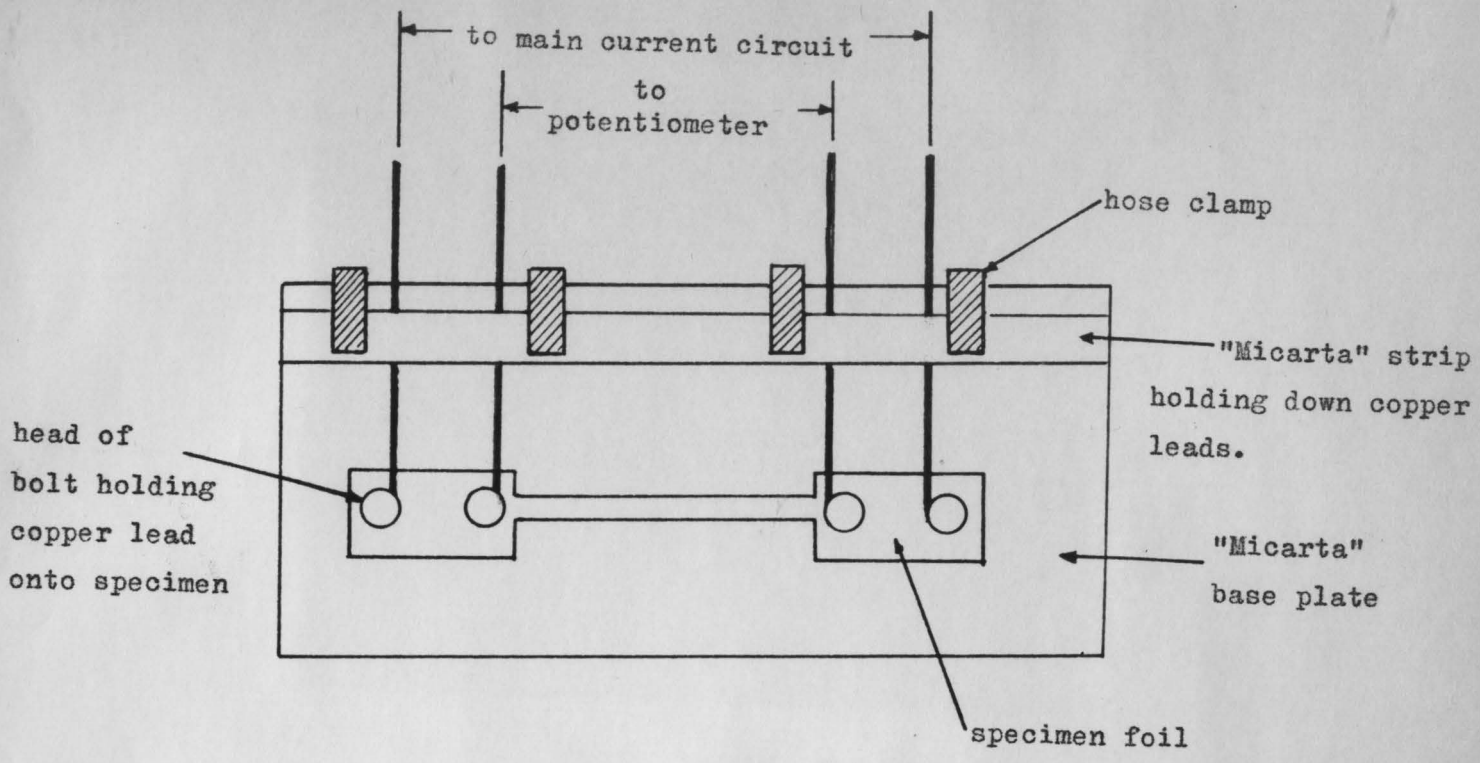

(a) PLAN VIEW. (Actual size).

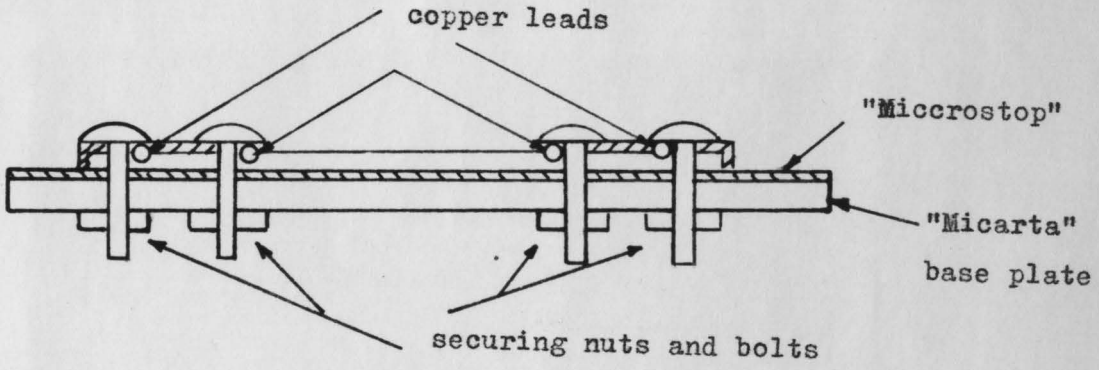

(b) CROSS SECTION THROUGH SPECIMEN. (Thickness exaggerated for clarity).

Fig. 1. Specimen mounting.

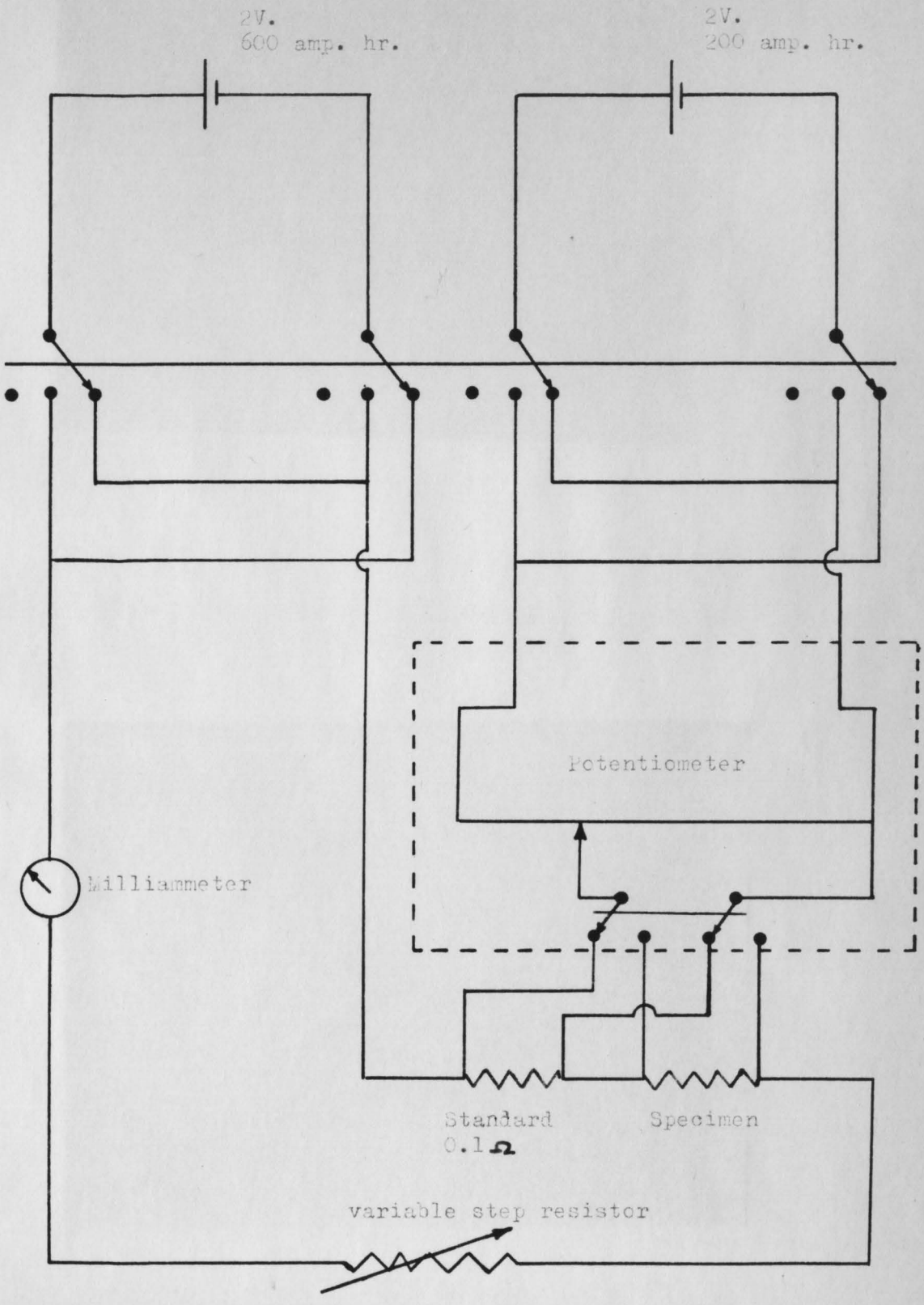

Fig. 2. Resistance measurement circuit.

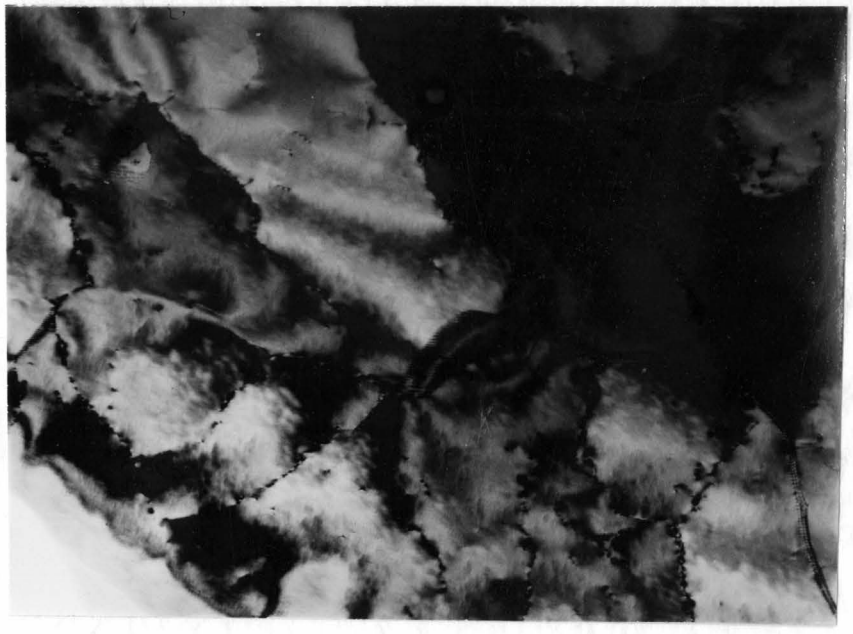

X 20,000

Fig. 3 (a). Transmission electron micrograph of cold-rolled foil prepared by electropolishing.

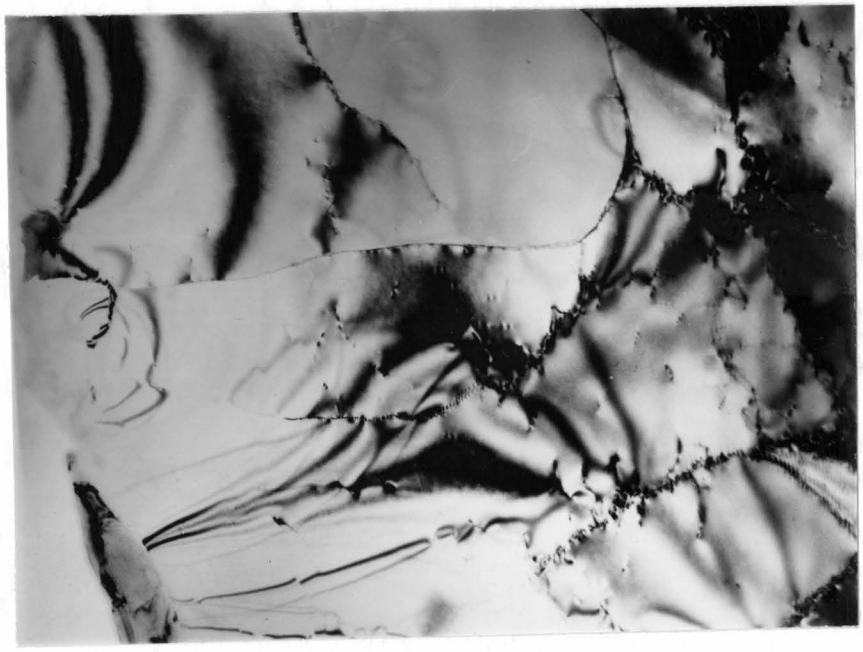

X 20,000

Fig. 3 (b). Transmission electron micrograph of cold-rolled foil prepared by electropolishing and etching 30min. in 2 gm./litre NaOH.

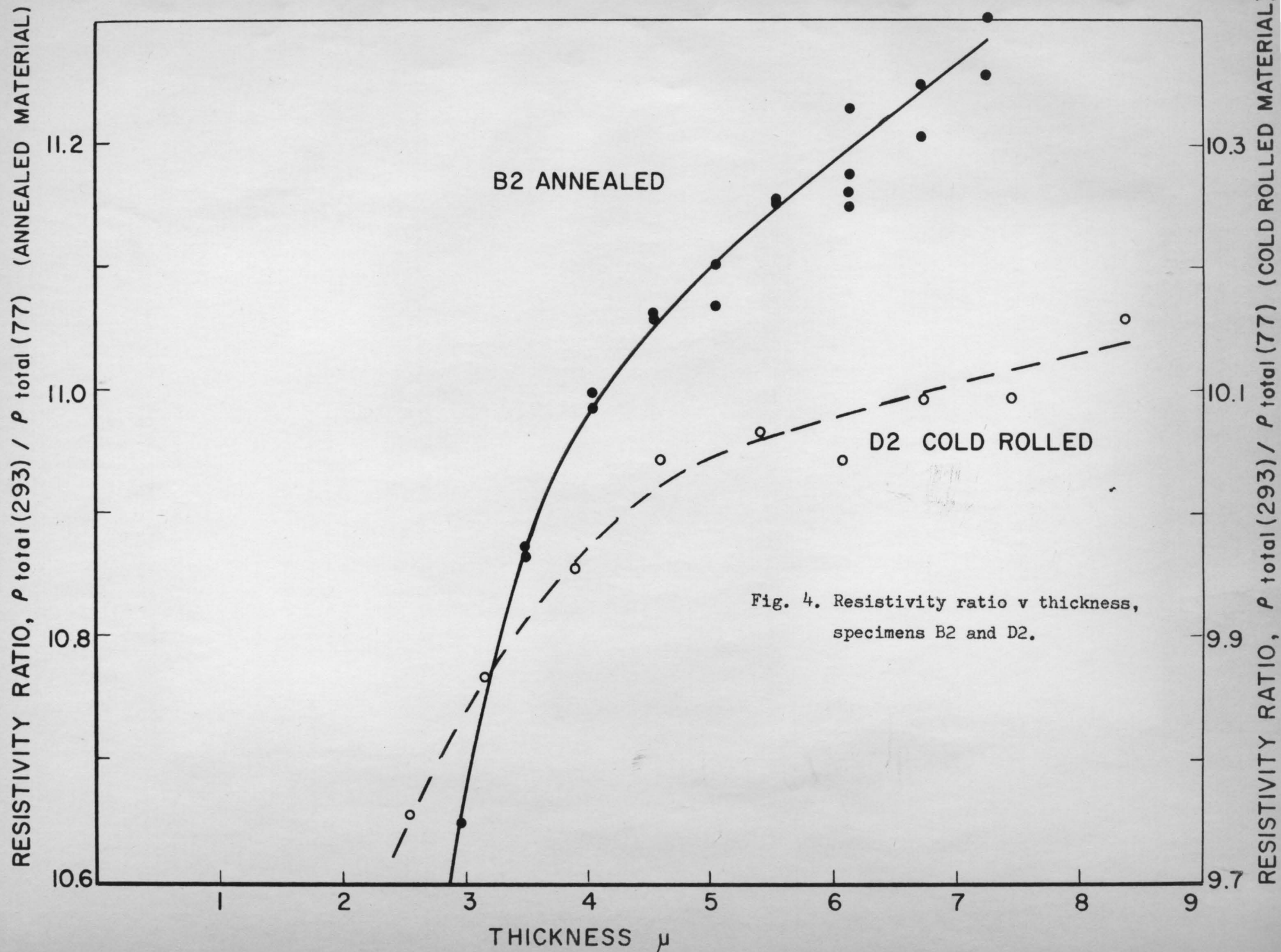

Fig. 4. Resistivity ratio v thickness, specimens B2 and D2.

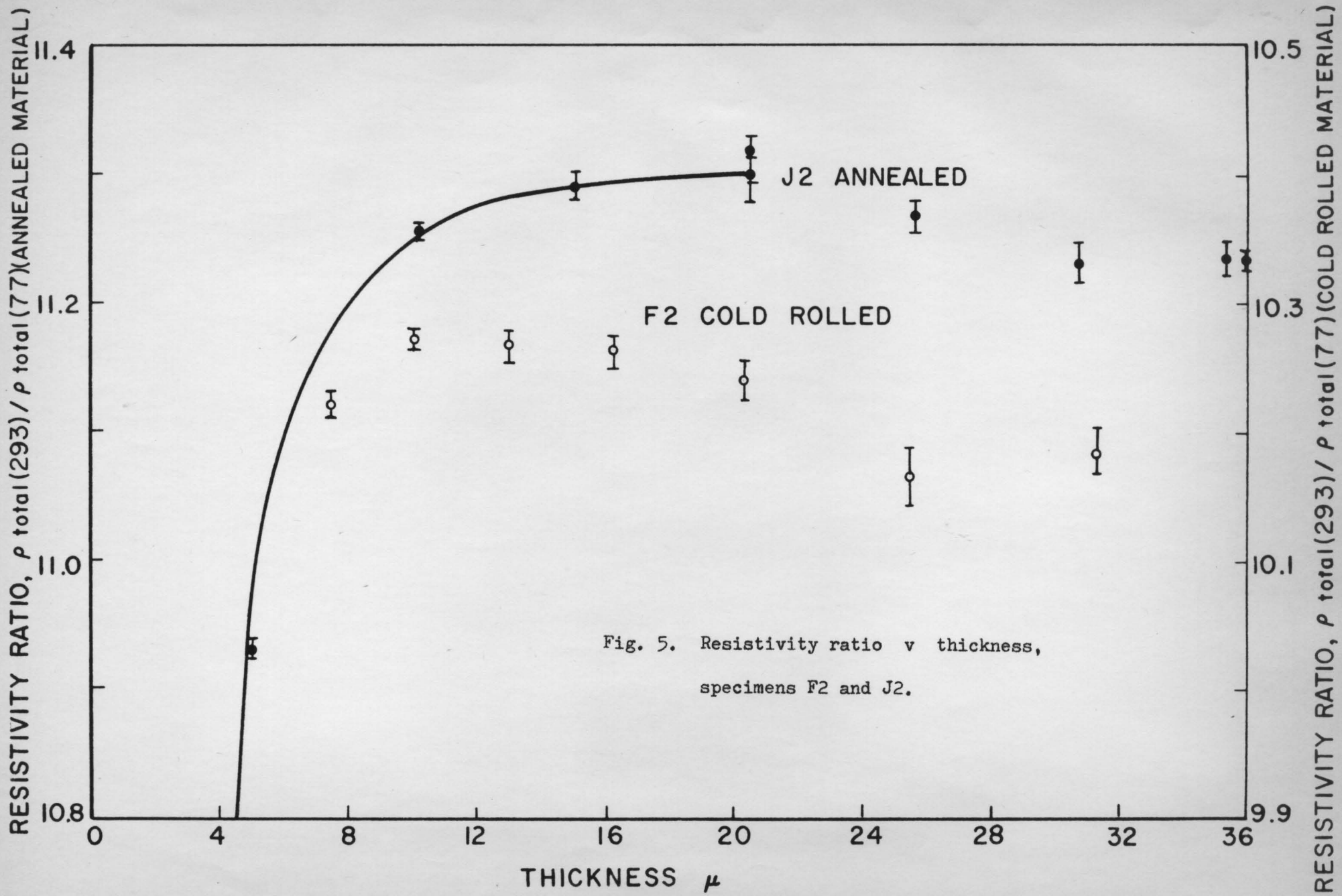

Fig. 5. Resistivity ratio v thickness, specimens F2 and J2.

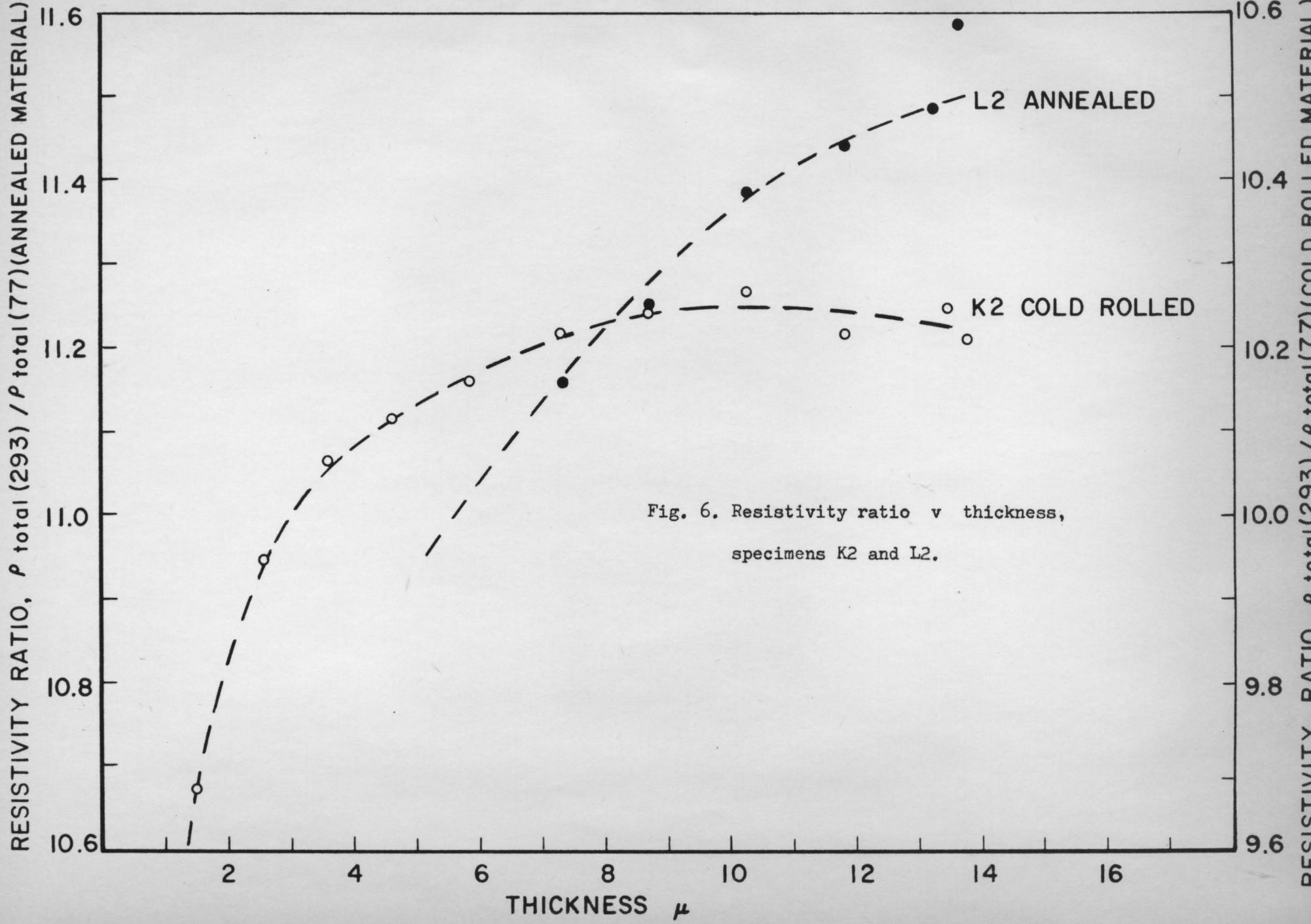

Fig. 6. Resistivity ratio v thickness, specimens K2 and L2.

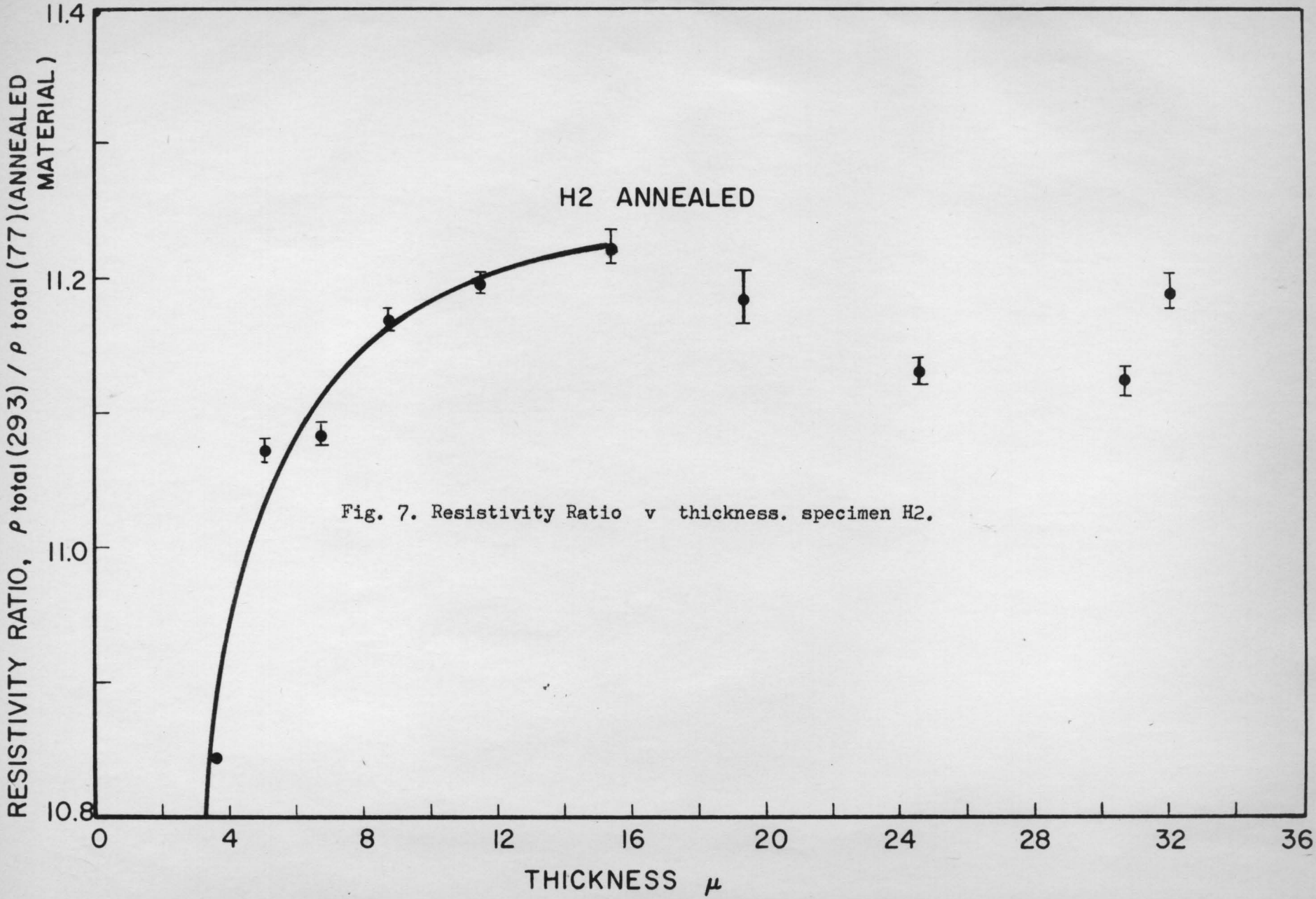

Fig. 7. Resistivity Ratio v thickness. specimen H2.

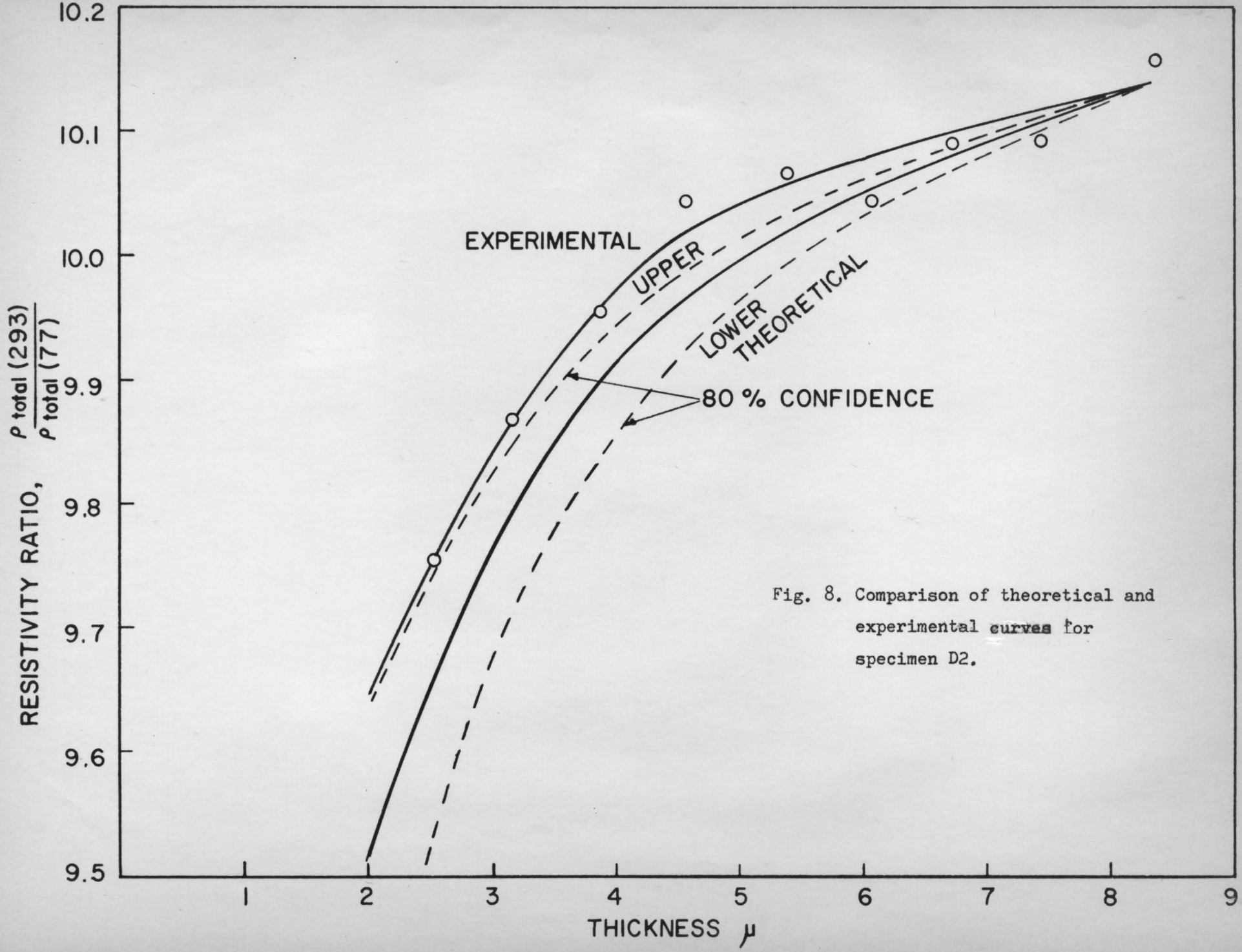

Fig. 8. Comparison of theoretical and experimental curves for specimen D2.

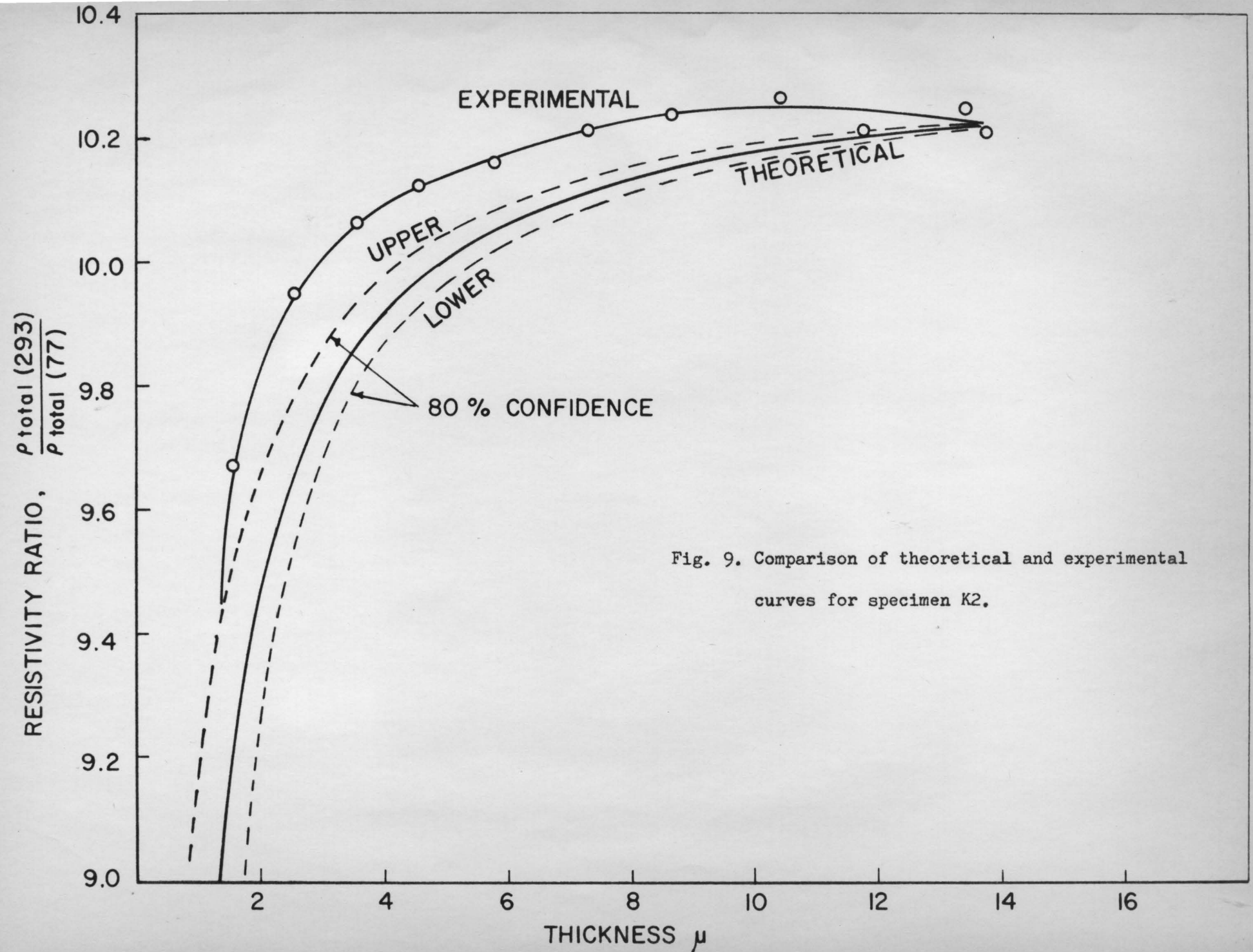

Fig. 9. Comparison of theoretical and experimental curves for specimen K2.

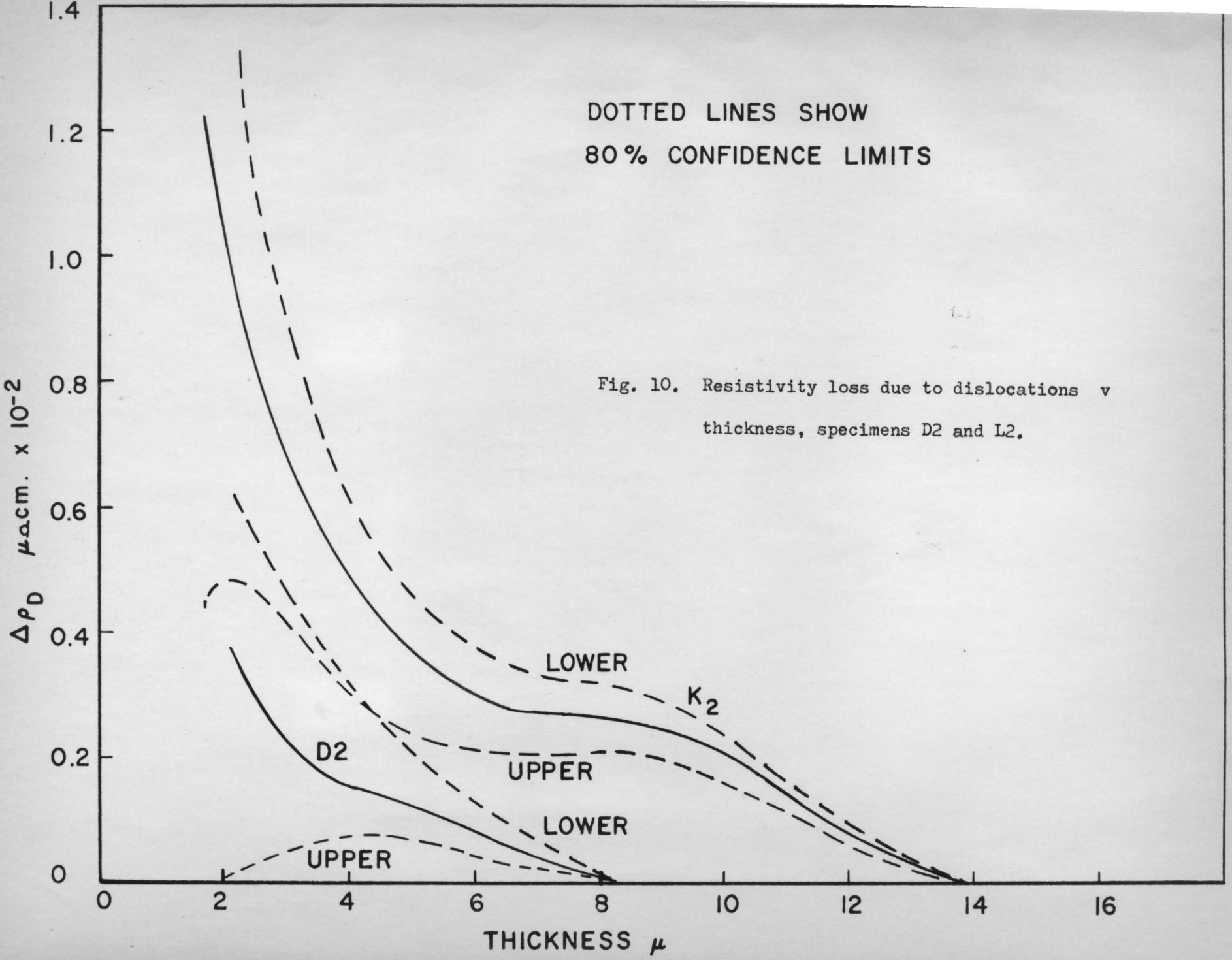

Fig. 10. Resistivity loss due to dislocations v thickness, specimens D2 and L2.

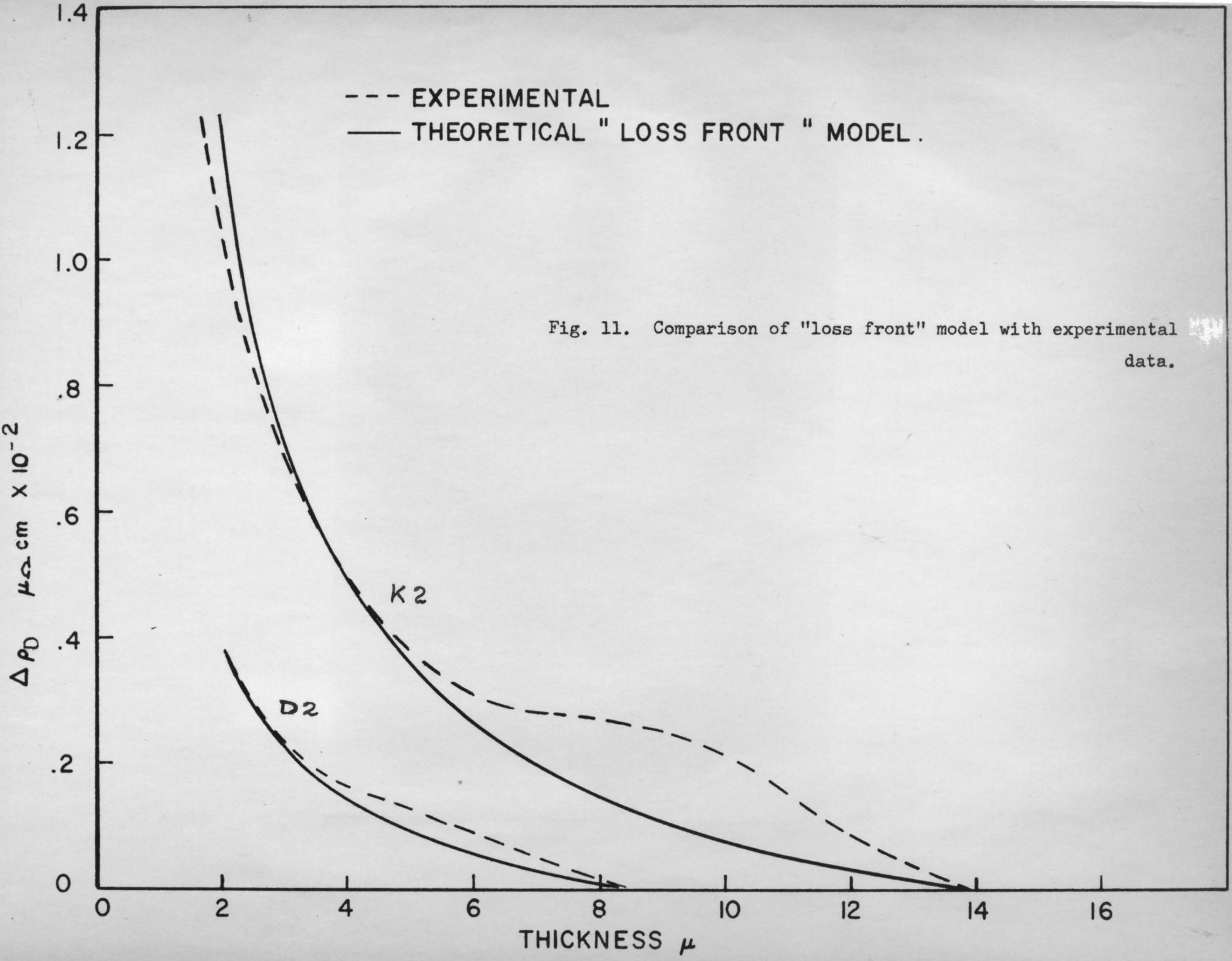

Fig. 11. Comparison of "loss front" model with experimental data.

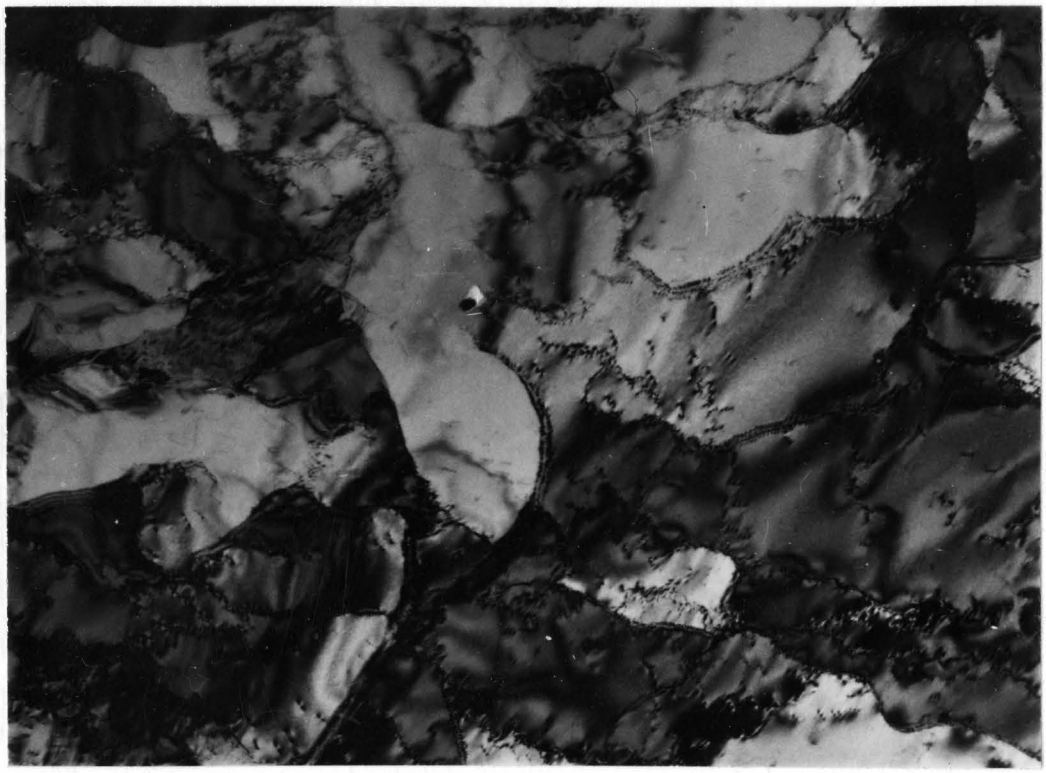

X 10,900

Fig. 12. Electron micrograph of cold-rolled foil, showing sub-grain size.